

Supplementary Information

One-pot Acid-Base Catalysed Tandem Reactions using a Bimodal N,S-doped Cubic Mesoporous Carbon

Hamzeh H. Veisi,^a Maryam Akbari,^a Babak Karimi,^{*a, b} Hojatollah Vali,^c Rafael Luque^{d, e}

a Department of Chemistry, Institute for Advanced Studies in Basic Sciences (IASBS), PO. Box 45195-1159, Prof. Sobouti Boulevard, Zanjan 45137-66731, Iran.

b Research Center for Basic Sciences & Modern Technologies (RBST), Institute for Advanced Studies in Basic Sciences (IASBS), Prof. Sobouti Boulevard, Zanjan 45137-66731, Iran.

c Department of Anatomy and Cell Biology and Facility for Electron Microscopy Research, McGill University, Montreal, Quebec H3A 2A7, Canada

d Peoples Friendship University of Russia (RUDN University), 6 Miklukho Maklaya str., 117198, Moscow, Russian Federation.

e Universidad ECOTEC, Km. 13.5 Samborondón, Samborondón, EC092302, Ecuador.

*Corresponding authors. E-mail: karimi@iasbs.ac.ir, luke_r@pfur.ru

Table of Contents

1	Experimental Procedures	5
1.1	Materials and instruments	5
1.2	Synthesis of the ordered mesoporous silica template (KIT-6)	5
1.3	Preparation of Ordered Mesoporous Silica (SBA-15)	6
1.4	Synthesis of 1-methyl-3-phenethyl-1 <i>H</i> -imidazolium hydrogen sulfate (MPIHS)	6
1.5	Measurement of ionic liquid density using a pycnometer	6
1.6	Synthesis of Ionic liquid-derived Bimodal cubic Ordered Mesoporous Carbon (IBOMC)	7
1.7	Synthesis of L-IBOMC material	7
1.8	Synthesis of H-IBOMC material	7
1.9	Synthesis of Br-IBOMC material	8
1.10	Preparation of Nitrogen-doped Ordered Mesoporous Carbon from Iran (NMCI)	8
1.11	Preparation of CMK-3	8
1.12	Preparation of CMK-8	9
1.13	General procedure for the catalytic Knoevenagel/deacetalization-Knoevenagel condensation reaction	9
1.14	General procedure for 5-HMF synthesis	9
1.15	Acidity and Basicity Measurements	11
2	Spectroscopic data for Knoevenagel/deacetalization-Knoevenagel condensation products	38
3	References	57

Schemes

Scheme S1: Schematic of the experimental procedure for the synthesis of IBOMC	13
---	----

Tables

Table S1: Characterization of carbocatalysts	12
Table S2: XRD Peak List of IBOMC and Recovered IBOMC	18
Table S3: CHNS of carbocatalyst	22
Table S4: Optimization of the reaction condition for the Knoevenagel condensation between benzaldehyde and malononitrile in the presence of IBOMC catalyst	23
Table S5: Optimization of the reaction condition for the Knoevenagel condensation between acetophenone and malononitrile in the presence of IBOMC catalyst	24
Table S6: The Knoevenagel condensation between ketones and malononitrile in the presence of IBOMC catalyst	25
Table S7: Optimization of the reaction condition for the deacetalization-Knoevenagel reaction between benzaldehyde dimethyl acetal and malononitrile in the presence of IBOMC catalyst	26
Table S8: Solvent optimization in fructose dehydration	27

Table S9: Catalyst optimization in fructose dehydration	27
Table S10: Solvent optimization for glucose dehydration.....	28
Table S11: Effect of H ₂ O and DMSO ratio in the queues phase of Dumesic solvent for glucose dehydration	28
Table S12: Dehydration of sucrose and cellulose	29
Table S13: Comparison between various catalysts in fructose dehydration.....	29
Table S14: Comparison between various carbocatalysts and IBOMC in dehydration of glucose at the same conditions.....	30

Figures

Figure S1: A) N ₂ sorption isotherm, B) Pore size distribution curve (evaluated using the BJH method)	13
Figure S2: TEM image of the KIT-6 as template	14
Figure S3: TEM images of IBOMC	15
Figure S4: FESEM images of IBOMC	17
Figure S5: XRD of KIT-6, IBOMC and Recovered IBOMC.....	18
Figure S6: Raman spectrum of IBOMC	19
Figure S7: Thermal gravimetric analysis of IBOMC under oxygen (left), and nitrogen (right) ...	19
Figure S8: FT-IR spectrum of IBOMC	20
Figure S9: XPS of IBOMC.....	20
Figure S10: C1s XPS spectrum of IBOMC	21
Figure S11: O1s XPS spectrum of IBOMC.....	21
Figure S12: Elemental mapping (C, N, O, and S elements) of IBOMC.....	22
Figure S13: NH ₃ and CO ₂ TPDs of Br-IBOMC	23
Figure S14: Porosimetry diagrams of recovered IBOMC	30
Figure S15: Thermal gravimetric analysis of recovered-IBOMC in dehydration of fructose into 5-HMF	31
Figure S16: Reusability chart of IBOMC catalyst in the Knoevenagel condensation of benzaldehyde and malononitrile	31
Figure S17: HPLC chromatogram of 5-HMF in Eurokat-H column.....	32
Figure S18: HPLC chromatogram of fructose in Eurokat-H column.....	32
Figure S19: HPLC chromatogram of glucose in Eurokat-H column	33
Figure S20: Detection of fructose through glucose dehydration with IBOMC as an acid-base bifunctional carbocatalyst	34
Figure S21: Detection of glucose through fructose dehydration with IBOMC as an acid-base bifunctional carbocatalyst	35
Figure S22: Fructose calibration curve. Stock solution included 0.051 g fructose in 3 mL H ₂ O, and every dilution was involved 50 µl of stock in 1 mL H ₂ O	36
Figure S23: Glucose calibration curve. Stock solution: 0.05 g glucose in 3 mL H ₂ O, and every dilution was involved 50 µl of stock in 1 mL H ₂ O.....	36
Figure S24: 5-HMF calibration curve-1. Stock solution included 0.036 g 5-HMF in 3.36 mL	

DMSO; every dilution was involved 50 μ l of solution in 1 mL H ₂ O.....	37
Figure S25: 5-HMF calibration curve-2. Stock solution included 0.0411 g 5-HMF in 1 mL H ₂ O; every dilution was involved 100 μ l of solution in 1 mL H ₂ O	37
Figure S26: ¹ H-NMR and ¹³ C-NMR spectra of the 2-benzylidenemalononitrile product in CDCl ₃	41
Figure S27: ¹ H-NMR and ¹³ C-NMR spectra of the 2-(4-nitrobenzylidene)malononitrile product in CDCl ₃	42
Figure S28: ¹ H-NMR and ¹³ C-NMR spectra of the 2-(4-cyanobenzylidene)malononitrile product in CDCl ₃	43
Figure S29: ¹ H-NMR and ¹³ C-NMR spectra of the 2-(3-bromobenzylidene)malononitrile product in CDCl ₃	44
Figure S30: ¹ H-NMR and ¹³ C-NMR spectra of the 2-(2,4-dichlorobenzylidene)malononitrile product in CDCl ₃	45
Figure S31: ¹ H-NMR and ¹³ C-NMR spectra of the 2-(4-methoxybenzylidene)malononitrile product in CDCl ₃	46
Figure S32 : ¹ H-NMR and ¹³ C-NMR spectra of the 2-(4-methylbenzylidene)malononitrile product in CDCl ₃	47
Figure S33: ¹ H-NMR and ¹³ C-NMR spectra of the 2-(naphthalen-1-ylmethylene)malononitrile product in CDCl ₃	48
Figure S34: ¹ H-NMR and ¹³ C-NMR spectra of the 2-(3-pyridylmethylene)malononitrile product in CDCl ₃	49
Figure S35: ¹ H-NMR and ¹³ C-NMR spectra of the 2-(furan-2-ylmethylene)malononitrile product in CDCl ₃	50
Figure S36: ¹ H-NMR and ¹³ C-NMR spectra of the 2-(1-phenylethylidene)malononitrile product in CDCl ₃	51
Figure S37: ¹ H-NMR and ¹³ C-NMR spectra of the 2-cyclopentylidenemalononitrile product in CDCl ₃	52
Figure S38: ¹ H-NMR and ¹³ C-NMR spectra of the 2-cyclohexylidenemalononitrile product in CDCl ₃	53
Figure S39: ¹ H-NMR and ¹³ C-NMR spectra of the 2-cycloheptylidenemalononitrile product in CDCl ₃	54
Figure S40: ¹ H-NMR spectrum (400 MHz, CDCl ₃) of 1-methyl-3-phenethyl- <i>1H</i> -imidazolium hydrogen sulfate (MPIHS).....	55
Figure S41: ¹³ C-NMR spectrum (100 MHz, DMSO-d ₆) of 1-methyl-3-phenethyl- <i>1H</i> -imidazolium hydrogen sulfate (MPIHS)	56
Figure S42: ¹ H-NMR spectrum (400 MHz, CDCl ₃) of 5-HMF	56
Figure S43: ¹³ C-NMR spectrum (100 MHz, CDCl ₃) of 5-HMF	57

1 Experimental Procedures

1.1 Materials and instruments

All chemicals including Pluronic P123 (EO₂₀PO₇₀EO₂₀, EO = ethylene oxide, PO= propylene oxide), tetraethyl orthosilicate (TEOS), *n*-butanol, 1-methylimidazole, 2-phenylethyl bromide, guanine, malononitrile, tetraethyl orthoformate, sulfuric acid (98%), hydrochloric acid (37%), hydrofluoric acid (48%) and also solvents were purchased from Merck and Sigma-Aldrich company. All the chemicals were used without further purification.

Philips CM-200 and Titan Krios transmission electron microscopes were utilized for studying the pore structure of the samples. The nitrogen adsorption-desorption isotherms were obtained using a Belsorp (BELMAX, Japan) analyzer at 77 K. All the samples were first degassed at 353 K for 10 h before the measurements. Specific surface area of the materials was determined from the linear part of the BET plot at the relative pressure range (P/P_0) of 0.05-0.15, and the pore size distribution (PSD) was calculated from the adsorption branch using the Barrett-Joyner-Halenda (BJH) method. Additionally, total pore volumes were assigned using the adsorbed volume at $P/P_0 \approx 0.995$. Surface morphology of the materials was investigated using a TeScan-Mira III ultrahigh resolution cold field emission scanning electron microscope (Fe-SEM). XPS spectra of the materials were recorded on Kratos Analytical X-ray photoelectron spectrometer. To correct possible deviation caused by electric charge, the C1s line at 285.0 eV was used as the internal standard. The main elemental composition was measured using vario-EL CHNS instrument. Thermogravimetric analysis (TGA) was performed using a NETZSCH STA 409 PC/PG instrument (Germany) at the temperature range of 25 to 800 °. Fourier transform infrared (FTIR) spectrum was attained by a Bruker vector 22 instrument in the range of 400 and 4000 cm⁻¹. High liquid chromatography analysis was achieved using the KNAUER system equipped with UV (K-2600) and RI (K-2301) detectors. NMR spectra were recorded using a Bruker instrument (¹H frequency: 400 MHz, ¹³C frequency: 100 MHz).

1.2 Synthesis of the ordered mesoporous silica template (KIT-6)

The KIT-6 template was prepared according to the procedure reported in literature.¹ Typically, 6 g of triblock copolymer P123 was dissolved in 220 g of deionized water and 12 g of hydrochloric acid (37 wt%) with stirring for 6 h at 35 °C. After complete dissolution, 6 g of *n*-butanol was added

into the solution at once and after 1 h of stirring, 12.48 g of TEOS was also added to it. The mixture was left under vigorous stirring for 24 h at 35 °C. Then, the mixture was placed under static condition at 100 °C for 24 h. The solid product obtained after the hydrothermal treatment was filtered and dried at 100 °C without washing. Finally, KIT-6 was obtained as a white solid by removing P123 through the calcination at 550 °C for 5 h under the air atmosphere.

1.3 Preparation of Ordered Mesoporous Silica (SBA-15)

Briefly, 24 g of Pluronic P123 was dissolved in 505 mL of H₂O and 101 mL of concentrated HCl at 35 °C. Consequently, tetraethyl orthosilicate (TEOS) (54.2 g) was added to the solution. The mixture was stirred vigorously at 35 °C for 20 h followed by an aging step at 80 °C for 24 h. The solid material was separated by filtration, washed with deionized water, and dried at room temperature. The surfactant was removed by solvent extraction with anhydrous ethanol in a Soxhlet apparatus for 24 h.²

1.4 Synthesis of 1-methyl-3-phenethyl-1H-imidazolium hydrogen sulfate (MPIHS)

Typically, a solution of dry toluene (50 mL), 1-methylimidazole (73.1 mmol), and 2-bromo-1-phenylethane (80.3 mmol) was refluxed for 24 h under an argon atmosphere. Then, the reaction mixture was allowed to cool at room temperature resulting in a two-phase solution. The separated ionic liquid (1-methyl-3-phenethyl-1H-imidazolium bromide) layer was washed with dry toluene and dry Et₂O and then dried under vacuum. 1-methyl-3-phenethyl-1H-imidazolium bromide (1 mmol) and H₂SO₄ (1 mmol) were added to a flask containing dry methylene chloride to perform the anion-exchange reaction. The resulting solution was refluxed for 48 h until all the hydrogen bromide by-product was removed. Finally, after evaporation of the solvent under vacuum, the MPIHS ionic liquid was isolated in good yield.

1.5 Measurement of ionic liquid density using a pycnometer

Measurement of the ionic liquid density was necessary to determine the amount of MPIHS required for filling all the pores of KIT-6 and therefore perform a perfect nanocasting. In this regard, the ionic liquid density was obtained using a pycnometer. Briefly, the pycnometer was first cleaned and dried carefully. Then, the weight of the pycnometer and the weight of the pycnometer filled with MPIHS were measured. The weight of MPIHS was obtained from the difference between two measured weights. The ionic liquid density was calculated by substituting the weight

of MPIHS and the known volume of the pycnometer into the density formula ($d = m/V$). It should be noted that density is a temperature-dependent parameter and the density obtained indicates the MPIHS density at room temperature. Hence, the following equation was used to determine the density of the ionic liquid at the temperature applied for the synthesis of IBOMC (100 °C). The approximate amount of the ionic liquid density at 100 °C was estimated to be 1.35 g.mL⁻¹ by substituting the density of water at 100 °C into the below equation ($d(\text{H}_2\text{O})=0.965 \text{ g.mL}^{-1}$).

$$\frac{m(\text{H}_2\text{O})}{d(\text{H}_2\text{O})} = \frac{m(\text{IL})}{d(\text{IL})}$$

1.6 Synthesis of Ionic liquid-derived Bimodal cubic Ordered Mesoporous Carbon (IBOMC)

IBOMC was obtained as follows: 2 g of the 1-methyl-3-phenethyl-1*H*-imidazolium hydrogen sulfate (MPIHS) ionic liquid and 0.3 g guanine were added to an HCl solution (5 mL, 2 M). This mixture was combined with 2 g of the degassed KIT-6 template and then stirred for 3h. The appropriate amount of the ionic liquid precursor was determined according to the total pore volume of KIT-6 and the MPIHS density. The resulting mixture was dried by increasing the temperature to 130 °C. The composite was then carbonized at 900 °C under an argon flow for 3 h. To remove the silica template, the obtained black powder was stirred in a solution of HF (3 M) for 24 h. The filtered mesoporous carbon was washed with deionized water several times and dried at 100 °C.

1.7 Synthesis of The L-IBOMC material

L-IBOMC was obtained as follows: 1.5 g MPIHS and 0.225 g guanine were added to an HCl solution (5 mL, 2 M). This mixture was combined with 2 g of the degassed KIT-6 template and then stirred for 3h. The resulting mixture was dried by increasing the temperature to 130 °C. The composite was then carbonized at 900 °C under an argon flow for 3 h. To remove the silica template, the obtained black powder was stirred in a solution of HF (3 M) for 24 h. The filtered mesoporous carbon was washed with deionized water several times and dried at 100 °C.

1.8 Synthesis of The H-IBOMC material

H-IBOMC was obtained as follows: 2.5 g MPIHS and 0.375 g guanine were added to an HCl solution (5 mL, 2 M). This mixture was combined with 2 g of the degassed KIT-6 template and then stirred for 3h. The resulting mixture was dried by increasing the temperature to 130 °C. The composite was then carbonized at 900 °C under an argon flow for 3 h. To remove the silica

template, the obtained black powder was stirred in a solution of HF (3 M) for 24 h. The filtered mesoporous carbon was washed with deionized water several times and dried at 100 °C.

1.9 Synthesis of The Br-IBOMC material

Br-IBOMC was obtained as follows: 2 g of the 1-methyl-3-phenethyl-1H-imidazol-3-ium bromide ionic liquid and 0.3 g guanine were added to an HCl solution (5 mL, 2 M). This mixture was combined with 2 g of the degassed KIT-6 template and then stirred for 3h. The appropriate amount of the ionic liquid precursor was determined according to the total pore volume of KIT-6 and the ionic liquid density. The resulting mixture was dried by increasing the temperature to 130 °C. The composite was then carbonized at 900 °C under an argon flow for 3 h. To remove the silica template, the obtained black powder was stirred in a solution of HF (3 M) for 24 h. The filtered mesoporous carbon was washed with deionized water several times and dried at 100 °C.

1.10 Preparation of Nitrogen-doped Ordered Mesoporous Carbon from Iran (NMCI)

The NMCI was prepared as follows: At first, 1 mL of MPIHS was heated at 100 °C and 0.15 g guanine was added slowly and the mixture was stirred until the dissolution of guanine in IL. In the next step, SBA-15 (1 g) was added slowly to form an SBA-15/IL paste. As described above, the final composite was transferred into the oven, and the carbonization procedure was performed under argon 5 L.min⁻¹ at 900 °C. Subsequently, the hard template was removed by dissolution in a sodium hydroxide (2 M) solution for 24 h at 50 °C. Filtration of the carbonized NMCI material and washing with deionized water up to neutralizing point and ethanol gives the final NMCI material in ~10 wt % yield with respect to the weight of IL and Guanine.³

1.11 Preparation of CMK-3

The template-free SBA-15 material was used as a mold for the synthesis of CMK-3 according to the literature.⁴ Typically, the resulted template-free SBA-15 was impregnated with an aqueous solution of sucrose (1.25 g of sucrose in 5 g of H₂O) containing 0.14 g of sulfuric acid and placed at 100 °C in a vacuum drying oven for 6 h. Consequently, the oven temperature was increased to 160 °C and maintained for 6 h, at that temperature to afford a dark brown or black powder. The impregnation step was repeated once with 0.8 g of sucrose. The resulted composite was then kept in an argon flow at 900 °C for 2 h to carbonize the sucrose. Afterward, to remove the silica

template, the generated black powder was stirred in a solution of ethanol and 1 M sodium hydroxide at 50 °C for 8 h. The CMK-3 carbon was afforded after filtration, washed several times with ethanol, and dried.

1.12 Preparation of CMK-8

The template-free KIT-6 material was used as a mold for the synthesis of CMK-8 according to the literature.¹ Typically, the resulted template-free KIT-6 was impregnated with an aqueous solution of sucrose (1.25 g of sucrose in 5 g of H₂O) containing 0.14 g of sulfuric acid and placed at 100 °C in a vacuum drying oven for 6 h. Consequently, the oven temperature was increased to 160 °C and maintained for 6 h to afford a dark brown or black powder. The impregnation step was repeated once with 0.8 g of sucrose. The resulted composite was then kept in an argon flow at 900 °C for 2 h to carbonize the sucrose. Afterward, to remove the silica template, the generated black powder was stirred in a solution of ethanol and 1 M sodium hydroxide at 50 °C for 8 h. The CMK-8 carbon was afforded after filtration, washed several times with ethanol, and dried.

1.13 General procedure for the catalytic Knoevenagel/deacetalization-Knoevenagel condensation reaction

The substrate (aldehyde, ketone, or acetal) (1 mmol), malononitrile (1.2 mmol), and IBOMC (5 mg in the case of aldehydes and 15 mg in the case of ketones and acetals) were placed into a flask. The resulting mixture was kept with stirring under the solvent-free condition at an appropriate temperature (room temperature in the case of aldehydes and 80 °C in the case of ketones and acetals). After completion of the reaction, 5 mL EtOH was added to the flask, and the catalyst was separated from the reaction mixture. Final products were further purified by recrystallization from EtOH.

1.14 General procedure for 5-HMF synthesis

In a 25 mL home-designed high-pressure Teflon-lined reactor, a mixture of carbohydrate (Merck) (0.277 mmol), catalyst (10-30 mg), and a single phase such as DMSO, isopropanol, H₂O (3 ml) or a biphasic solvent comprising DMSO, H₂O/2-butanol, methyl isobutyl ketone (0.7, 0.3 / 0.6, 1.4 ml) was prepared. The sealed reactor was then placed in an oil bath at 140 to 180 °C. After completing the reaction, the carbocatalyst was filtered, and the consequent solution was investigated by HPLC for HMF yield and conversion calculation.

Reaction samples were analyzed by the KNAUER High Performance Liquid Chromatography (HPLC) system equipped with UV (K-2600) and RI (K-2301) detectors. Sugars were monitored with a Eurokat H (C-54-1181H) column, using H₂SO₄ (5 mM) as the mobile phase with a flow rate of 1 mL.min⁻¹ and a column temperature of 333 K. Also, 5-HMF was measured for the organic and aqueous phases with a Nucleosil-100 (C18) column, using a 7:3 v/v (H₂O: CH₃CN) gradient at a flow rate of 0.6 mL.min⁻¹ and a column temperature of 303 K with a UV detector (282 nm). It was presumed that the changes of volume are negligible after the reaction for all experiments. Conversion of carbohydrates was determined as moles of hexose or pentose reacted per mole of carbohydrate fed according to an external standard. Also, 5-HMF yield was determined as moles of 5-HMF produced based on 5-HMF external standard. Conversions of cellulose were determined according to the wt% of the consumed substrate. For this purpose, after the reaction, the unreacted substrate was filtered, thoroughly washed, and dried to constant weight.

Calculation of conversion and yield for biphasic reactions

To calculate the carbohydrate conversion in biphasic reaction systems, 100 μL of the aqueous phase was diluted in 1 mL H₂O and then examined by using a Eurokat H (C-54-1181H) column, an aqueous solution of H₂SO₄ (5 mM) as the mobile phase with a flow rate of 0.8 mL.min⁻¹ and a column temperature of 30 °C through an RI detector. To estimate 5-HMF yield in biphasic system, 10 μL organic or aqueous phases separately were diluted in in a solution of water and acetonitrile (7:3 v/v), and evaluated by using a Nucleosil-100 (C18) column, with a 7:3 v/v of water and CH₃CN as a mobile phase at a flow rate of 0.6 mL.min⁻¹ and a column temperature of 30 °C through a UV detector (282 nm).

Calculation of conversion and yield for single phase reactions

To determine carbohydrate conversion in a single solvent system, 20 μL of mixture was analyzed by using a Eurokat H (C-54-1181H) column, H₂SO₄ (5 mM) as the mobile phase at a flow rate of 0.8 mL.min⁻¹ and a column temperature of 30 °C. To calculate the 5-HMF yield in the single phase systems, 100 μL of the mixture was diluted with 1 mL of H₂O and then analyzed through the same method as explained for organic phase analysis in biphasic systems.

It was presumed that the changes of volume are negligible after the reactions for all experiments. Carbohydrate conversion was determined as moles of reacted carbohydrate per mole of carbohydrate-fed according to external carbohydrate standard. Also, 5-HMF yield was determined as moles of 5-HMF produced according to the external standard of 5-HMF. Conversions of

cellulose were determined according to the wt% of the consumed substrate. For this purpose, after the reaction, the unreacted substrate was filtered, thoroughly washed, and dried to constant weight.

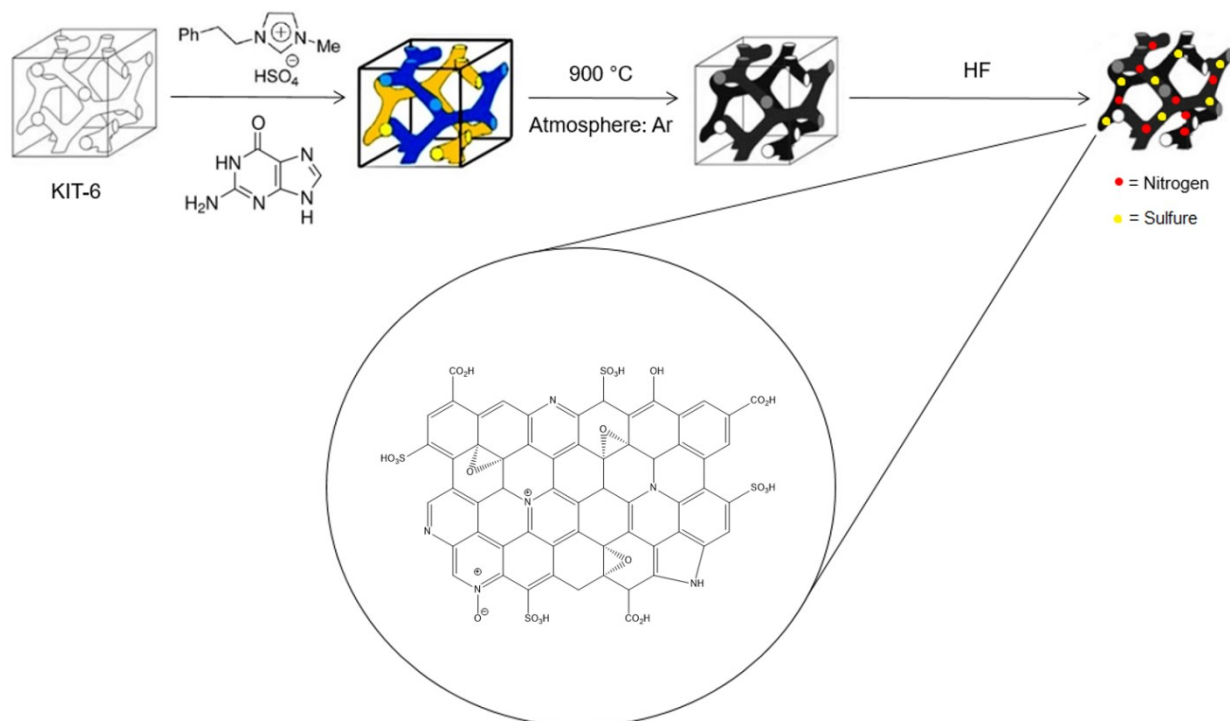
1.15 Acidity and Basicity Measurements

To evaluate the amount of the acidic sites on carbon materials, the back titration technique has been performed with a standard hydrochloric acid solution in the presence of the phenolphthalein indicator has been performed. Also, the existence of basic sites has been assessed with acid-base titration using a standard sodium hydroxide solution and phenolphthalein indicator. In addition, the temperature-programmed desorption (TPD) of carbon dioxide and ammonia was carried out with an Autochem II chemisorption analyzer (Micromeritics, 2920) to assess the strength and exact amount of the basic and acidic sites, respectively. Before examination, the samples were exposed to heat-treatment at 200 °C for 1 h under a Helium atmosphere. When the temperature was decreased to 50 °C, the samples were soaked by carbon dioxide for 1 h, and then the gas was changed to Helium to eliminate the physisorbed carbon dioxide molecules until the baseline was flat. Then, the temperature was increased to 800 °C (heating rate: 10 mL.min⁻¹) to obtain the CO₂-TPD curves. In the same manner for NH₃-TPD, the samples were preheated at 200 °C for 1 h under a flow of Helium gas at a rate of 30 mL.min⁻¹ and chilled to 100 °C. Ammonia gas was adsorbed using 10% NH₃ in He for 1 h. Desorption process was performed by increasing temperature from 100 to 800 °C with the rate of 10 °C.min⁻¹ under a flow of He gas at the rate of 30 mL.min⁻¹. The NH₃ and CO₂ desorption profiles of different carbon samples are shown in Figure S10.

Table S1: Characterization of carbocatalysts

Entry	Material	Topology (symmetrical structure)	S_{BET} ($\text{m}^2 \cdot \text{g}^{-1}$) ^a	V_t ($\text{cm}^3 \cdot \text{g}^{-1}$) ^b	r_p BJH (nm) ^c	N% ^d	Acidity ($\text{mmol} \cdot \text{g}^{-1}$) ^e	Basicity ($\text{mmol} \cdot \text{g}^{-1}$) ^f
1	KIT-6	Cubic (<i>Ia3d</i>)	1103	1.33	3.53	-	-	-
2	IBOMC ^g	Cubic (<i>Ia3d</i>)	965	1.18	7.89/1.85 ^j	11.20	1.01 (0.8 ^k)	0.45 (0.4 ^k)
3	L- IBOMC ^h	Cubic (<i>Ia3d</i>)	818	1.12	4.6/1.85 ^j	-	-	-
4	H- IBOMC ⁱ	Cubic (<i>Ia3d</i>)	452	0.716	5.28/1.64 ^j	-	-	-
5	Br- IBOMC	Cubic (<i>Ia3d</i>)	856	1.58	6/1.85 ^j	11	0.4	0.42
6	CMK-8	Cubic (<i>Ia3d</i>)	768	0.937	1.85	-	0.23	-
7	NMCI	Hexagonal (<i>p6mm</i>)	768	0.629	1.21	12.6	1.30	0.79
8	Carbon Active	Disorder	647	0.570	1.21	0.0	0.58	-
9	Recovered IBOMC ^l	Cubic (<i>Ia3d</i>)	577	0.89	1.21	9.11	-	-

^a S_{BET} = specific surface area, ^b V_t = total pore volume, ^c D_{BJH} = pore size distribution calculated from the adsorption branch using BJH methods, ^d Calculated from elemental (CHNS) analysis, ^e Calculated by NH_3 -TPD analysis, ^f Calculated by CO_2 -TPD analysis, ^g The amount of MPIHS ($\text{cm}^3 \cdot \text{g}^{-1}$)/ V_t of KIT-6 ($\text{cm}^3 \cdot \text{g}^{-1}$) = 1, ^h The amount of MPIHS ($\text{cm}^3 \cdot \text{g}^{-1}$)/ V_t of KIT-6 ($\text{cm}^3 \cdot \text{g}^{-1}$) < 1, ⁱ The amount of MPIHS ($\text{cm}^3 \cdot \text{g}^{-1}$)/ V_t of KIT-6 > 1, ^j D_{DH} = pore size distribution calculated from the adsorption branch using DH methods, ^k Calculated by back titration, ^l Recovered IBOMC in dehydration of fructose into 5-HMF.



Scheme S1: Schematic of the experimental procedure for the synthesis of IBOMC

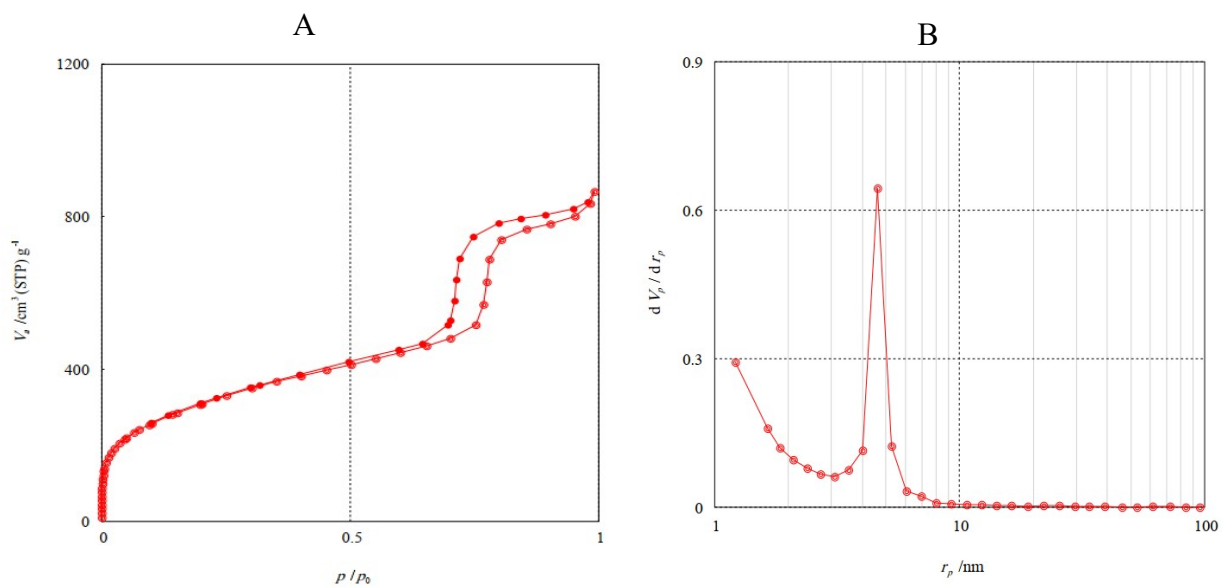


Figure S1: A) N₂ sorption isotherm, B) Pore size distribution curve (evaluated using the BJH method)

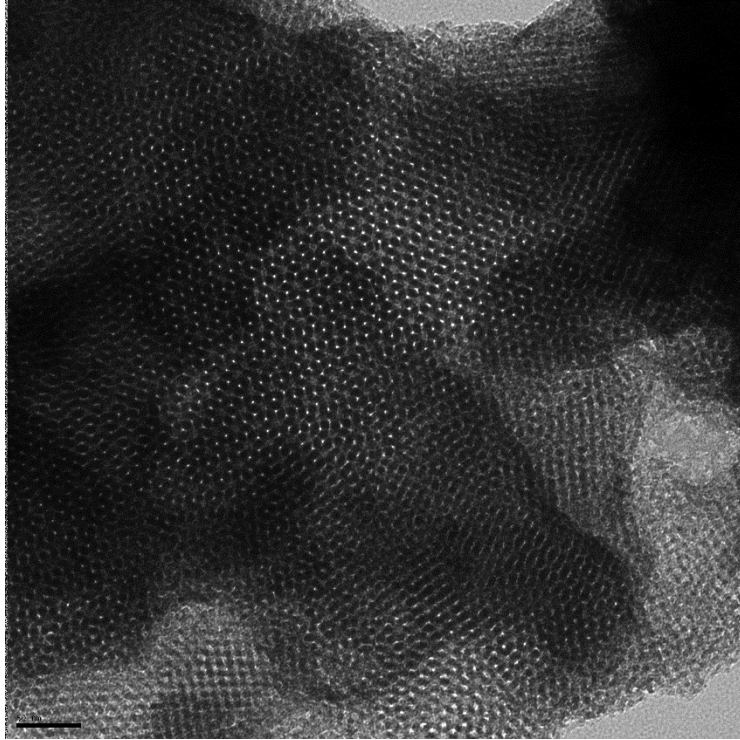
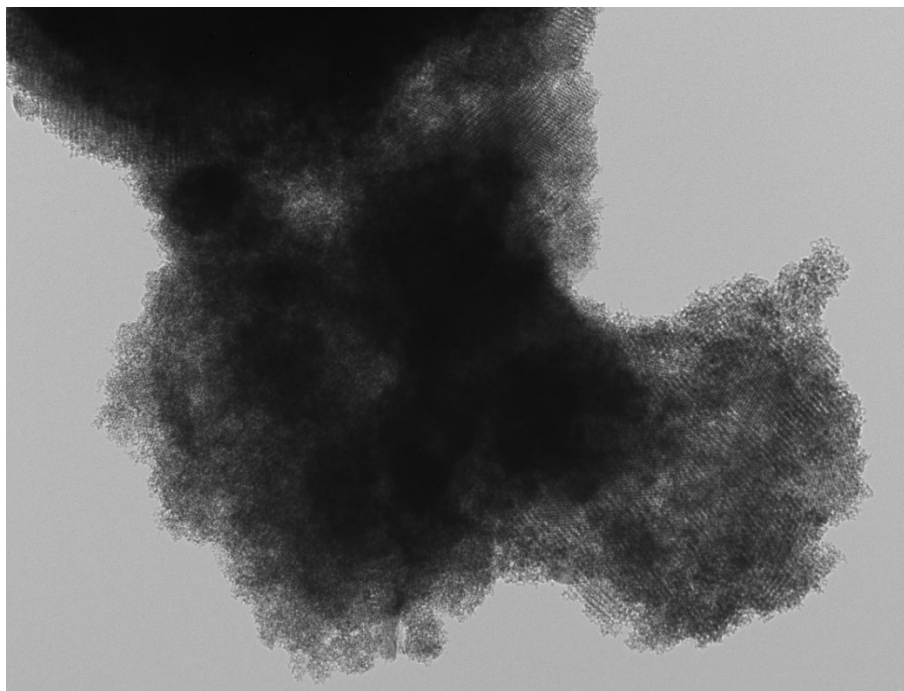
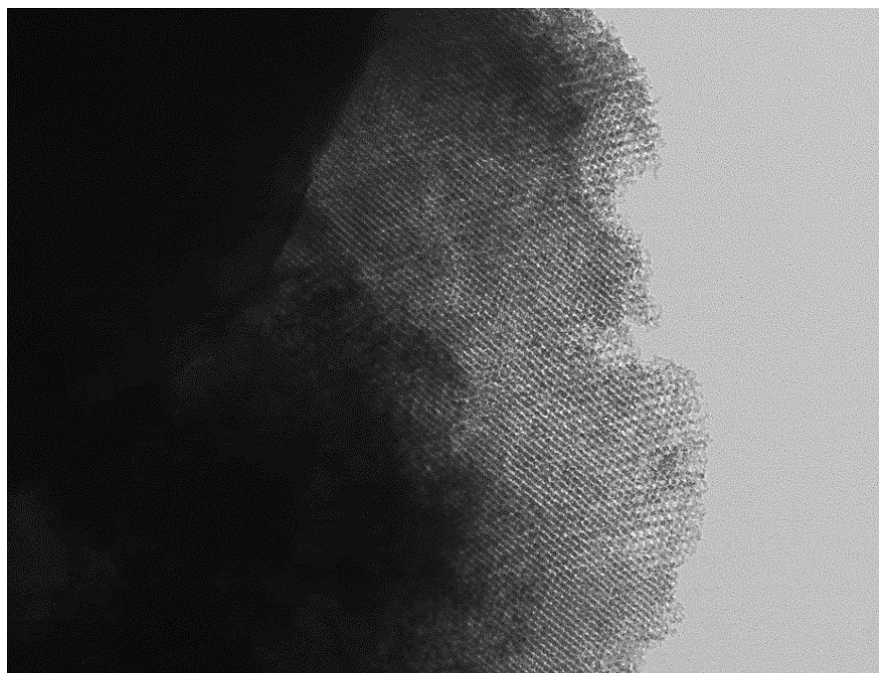


Figure S2: TEM image of the KIT-6 as template



Ma-2-3-23k.tif
Cal: 0.755287 nm/pix
12:09:15 p 06/14/14

100 nm
HV=120.0kV
Direct Mag: 23000x
FEMR

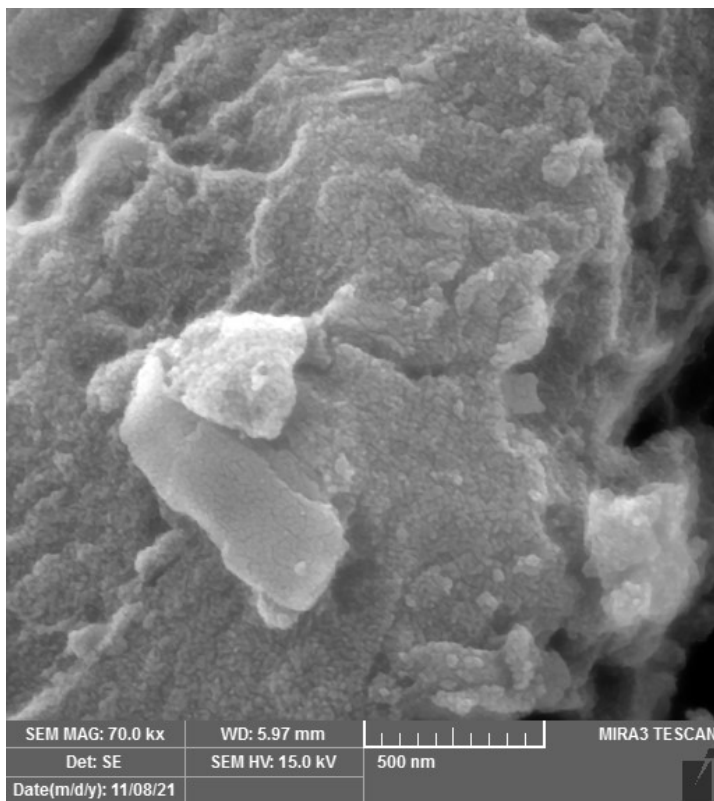
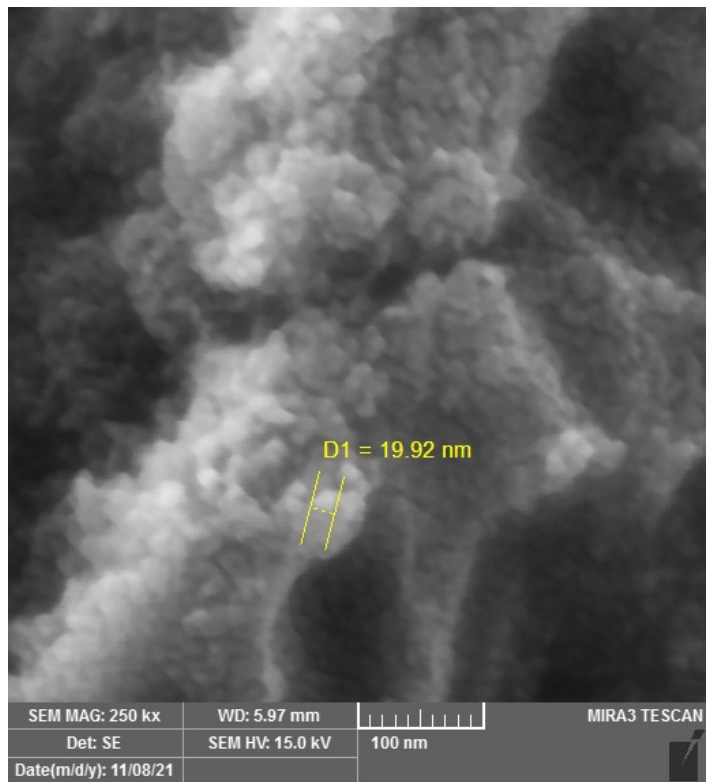


8.tif
Cal: 0.35461 nm/pix
9:55:36 a 01/07/16

100 nm
HV=120.0kV
Direct Mag: 49000x
FEMR



Figure S3: TEM images of IBOMC



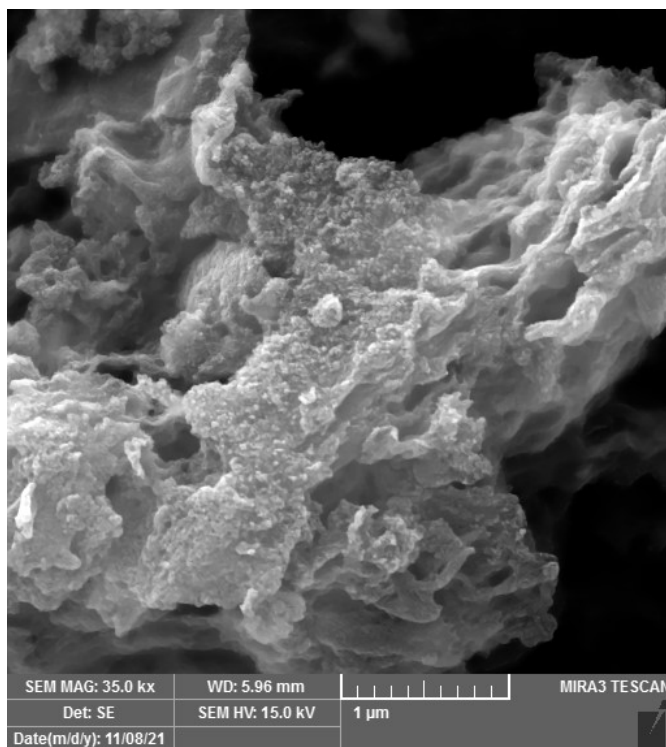


Figure S4: FESEM images of IBOMC

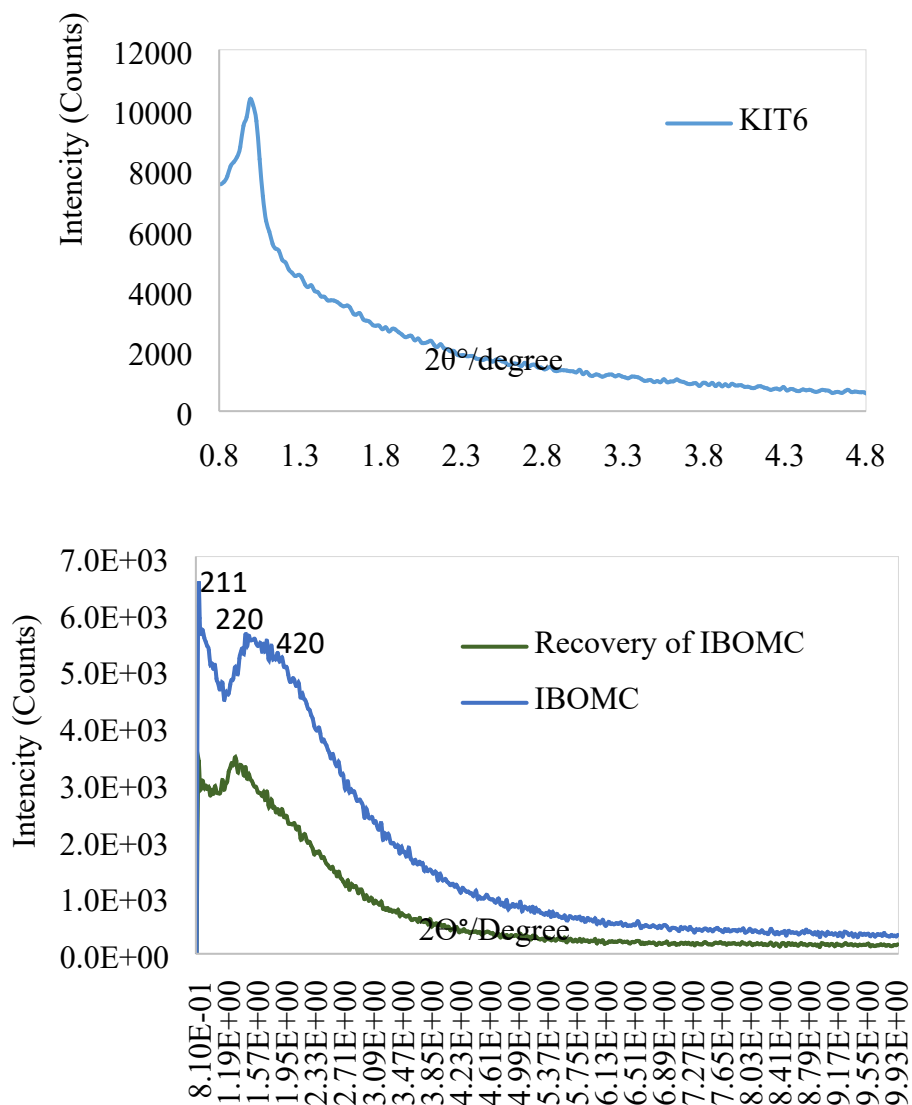


Figure S5: XRD of KIT-6, IBOMC and Recovered IBOMC

Table S2: XRD Peak List of IBOMC and Recovered IBOMC

Material	Pos.[°2Th.]	Height [cts]	d-spacing [Å]	Rel. Int. [%]
IBOMC	1.8 (2)	755 (873)	49.47	100.00
Re-IBOMC ^a	1.31(5)	744(2396)	67.27929	100.00

^a Recovered IBOMC from dehydration reaction of fructose into 5-HMF



Figure S6: Raman spectrum of IBOMC

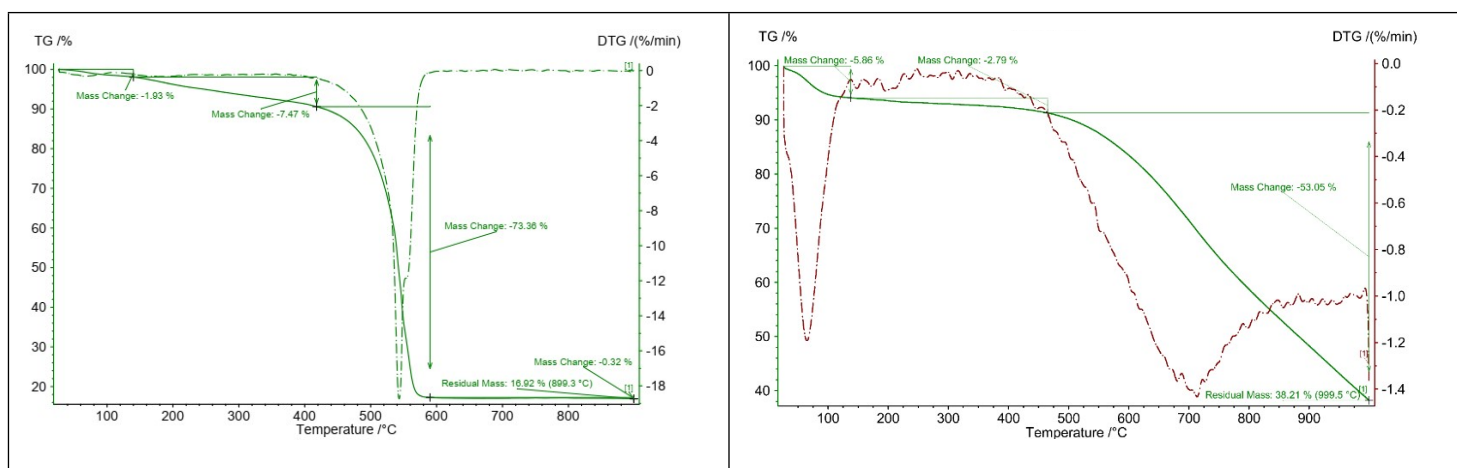


Figure S7: Thermal gravimetric analysis of IBOMC under oxygen (left), and nitrogen (right)

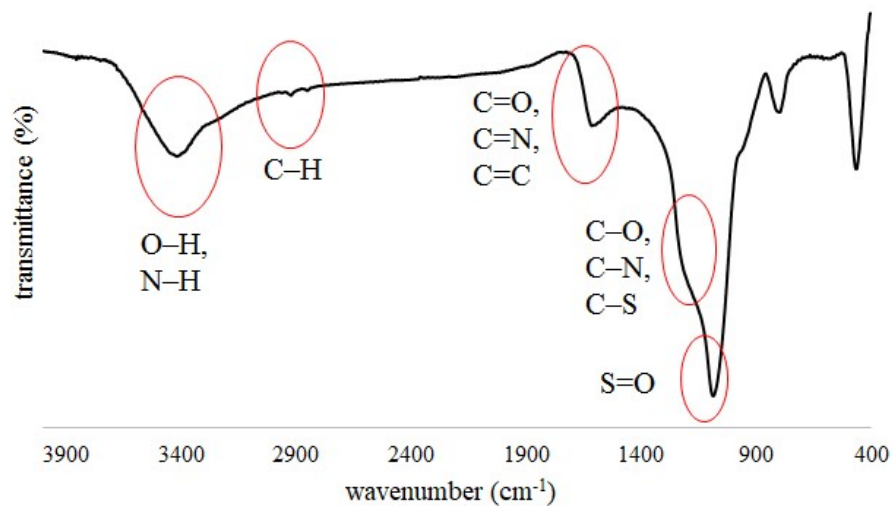


Figure S8: FT-IR spectrum of IBOMC

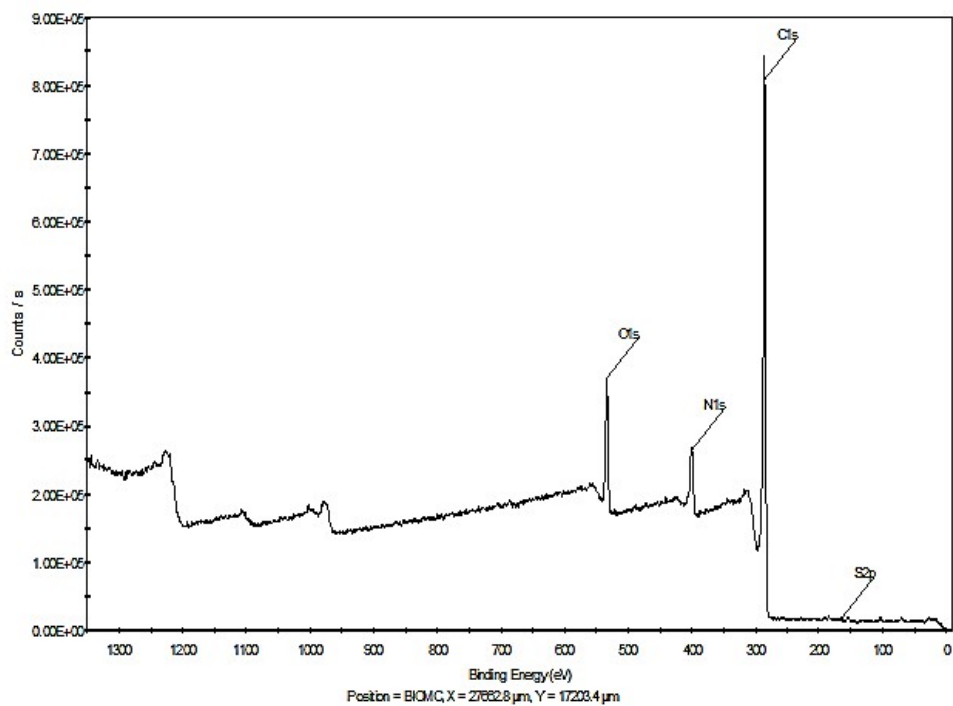


Figure S9: XPS of IBOMC

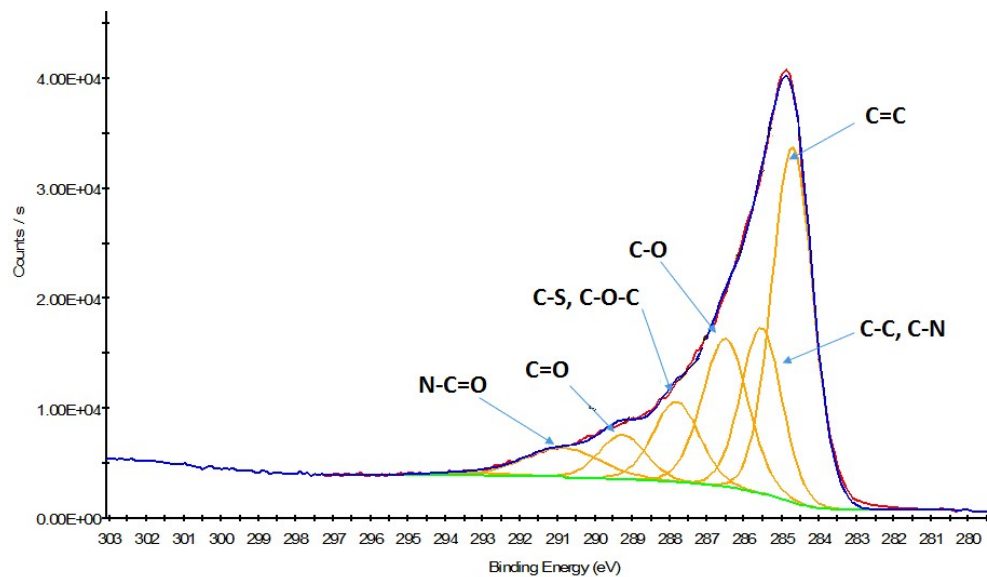


Figure S10: C1s XPS spectrum of IBOMC

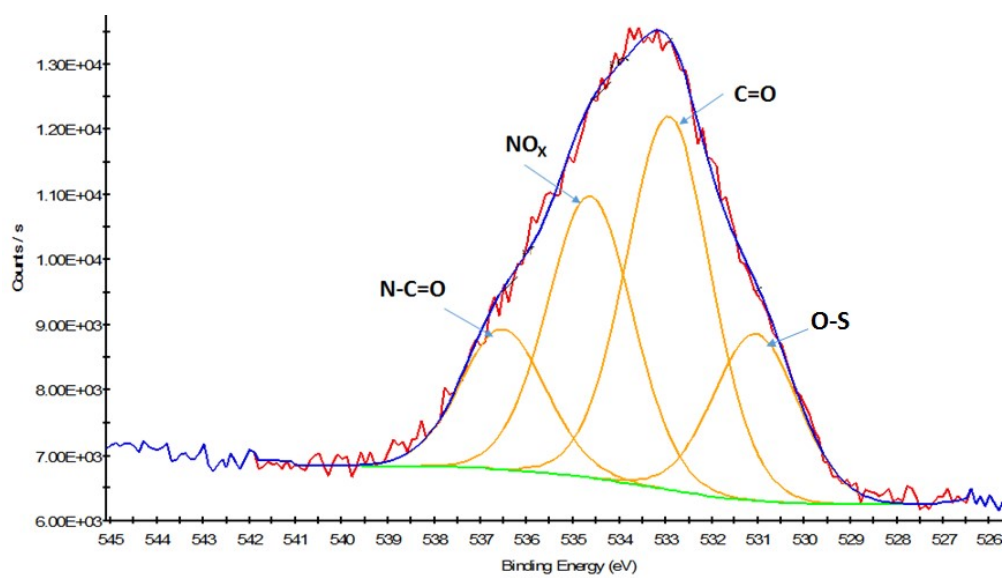


Figure S11: O1s XPS spectrum of IBOMC

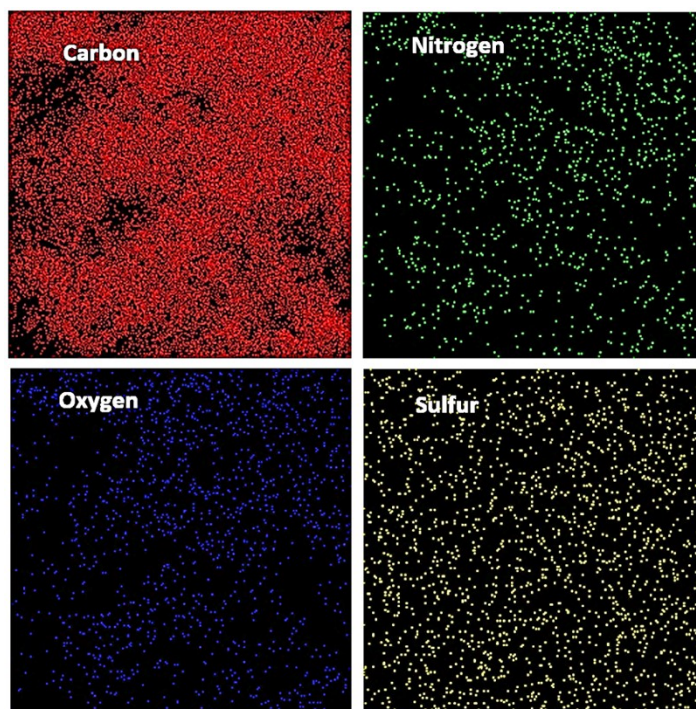


Figure S12: Elemental mapping (C, N, O, and S elements) of IBOMC

Table S3: CHNS of carbocatalyst

Entry	Carbon%	Nitrogen%	Sulfur%	Hydrogen%
IBOMC	70	11.2	1.91	0.616
Recovered-IBOMC ^a	63.4	9.12	1.43	0.496

^a Recovered IBOMC in dehydration of fructose into 5-HMF

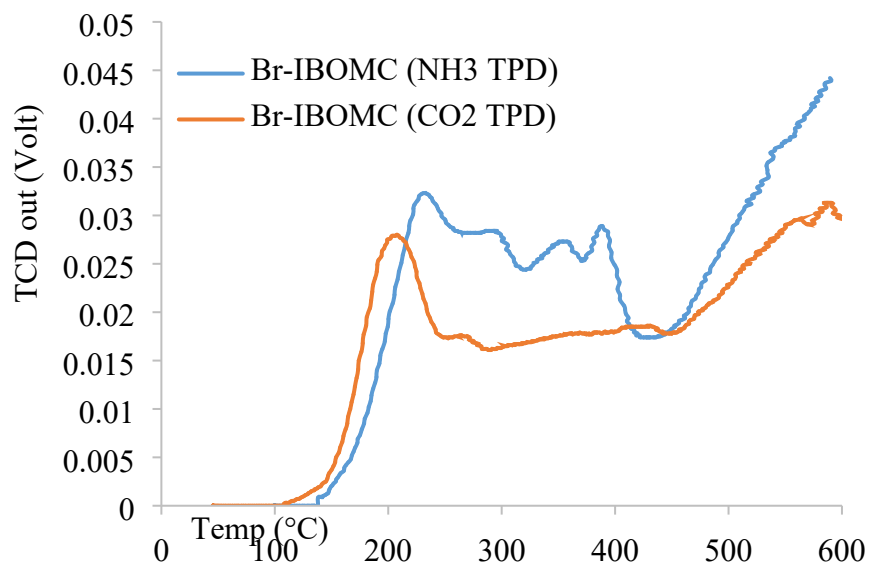
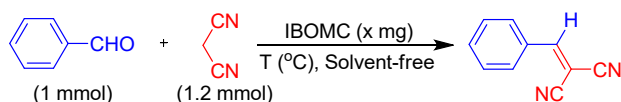


Figure S13: NH₃ and CO₂ TPDs of Br-IBOMC

Table S4: Optimization of the reaction condition for the Knoevenagel condensation between benzaldehyde and malononitrile in the presence of IBOMC catalyst

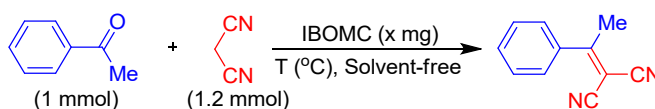


Entry	Catalyst (mg)	T (°C)	Time	Yield (%) ^{a,b}
1	30	80	24 h	100
2	30	60	24 h	100
3	25	60	24 h	100
4	25	r.t.	24 h	100
5	15	r.t.	24 h	100
6	10	r.t.	24 h	100
7	5	r.t.	24 h	100
8	3	r.t.	24 h	82
9	5	r.t.	12 h	100
10	5	r.t.	6 h	100
11	5	r.t.	4 h	100
12	5	r.t.	2 h	100
13	3	r.t.	1 h	100
14	5	r.t.	30 min	100
15	5	r.t.	15 min	94

16	5	r.t.	10 min	91
----	---	------	--------	----

^a Reaction conditions: Substrates (1 mmol), Malononitrile (1.2 mmol), IBOMC (X mg), T °C, solvent free condition. ^b Isolated yield by flash chromatography and/or recrystallization from EtOH.

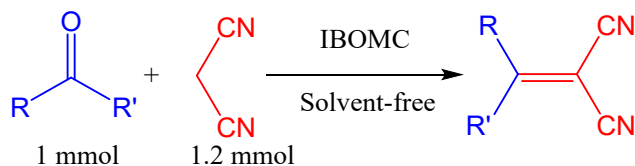
Table S5: Optimization of the reaction condition for the Knoevenagel condensation between acetophenone and malononitrile in the presence of IBOMC catalyst



Entry	Catalyst (mg)	T (°C)	Time	Yield (%) ^{a,b}
1	5	r.t.	24 h	45
2	10	r.t.	24 h	63
3	15	r.t.	24 h	76
4	25	r.t.	24 h	54
5	5	60	24 h	62
6	10	60	24 h	70
7	15	60	24 h	67
8	5	80	24 h	76
9	10	80	24 h	80
10	15	80	24 h	90
11	5	100	24 h	76
12	5	100	24 h	77
13	15	80	12 h	90
14	15	80	10 h	90
15	15	80	8 h	90
16	15	80	7 h	63

^a Reaction conditions: Substrates (1 mmol), Malononitrile (1.2 mmol), IBOMC (X mg), T °C, solvent free condition. ^b Isolated yield by flash chromatography and/or recrystallization from EtOH.

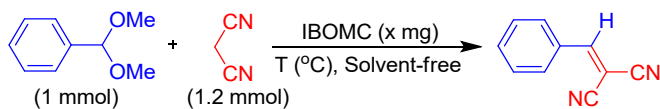
Table S6: The Knoevenagel condensation between ketones and malononitrile in the presence of IBOMC catalyst



Entry	Substrate	Catalyst (mg)	T (°C)	Time	Yield (%) ^{a,b}
1	Acetophenone	5	r.t.	24 h	45
2	Acetophenone	10	r.t.	24 h	63
3	Acetophenone	15	r.t.	24 h	76
4	Acetophenone	25	r.t.	24 h	54
5	Acetophenone	15	60	24 h	67
6	Acetophenone	15	80	24 h	90
7	Acetophenone	5	100	24 h	77
8	Acetophenone	15	80	12 h	90
9	Acetophenone	15	80	8 h	90
10	Acetophenone	15	80	7 h	63
11	Cyclopentanone	15	80	8 h	82
12	Cyclohexanone	15	80	5 h	88
13	Cycloheptanone	15	80	6.5 h	84

^a Reaction conditions: Substrates (1 mmol), Malononitrile (1.2 mmol), IBOMC (15 mg), 80 °C, solvent free condition. ^b Isolated yield by flash chromatography and/or recrystallization from EtOH.

Table S7: Optimization of the reaction condition for the deacetalization-Knoevenagel reaction between benzaldehyde dimethyl acetal and malononitrile in the presence of IBOMC catalyst



Entry	Catalyst (mg)	T (°C)	Time	Yield (%) ^a
1	30	80	24 h	100
2	15	80	24 h	100
3	12	80	24 h	83
4	15	60	24 h	68
5	15	r.t.	24 h	6
6	15	80	12 h	100
7	15	80	10 h	100
8	15	80	8 h	100
9	15	80	4 h	98
10	15	80	3 h	81

^aIsolated yield by flash chromatography and/or recrystallization from EtOH.

Table S8: Solvent optimization in fructose dehydration

Entry	Solvent (3 mL)	Conversion (%) ^a	HMF yield (%) ^a	Selectivity (%)
1	H ₂ O	100	13	13
2	H ₂ O:MIBK (1:2)	46	18	39
3	H ₂ O: Choline Chloride: MIBK (1:1:2)	78	16.5	21
4	Dumesic Solvent [H ₂ O:DMSO (0.3:0.7) mL / 2-butanol:MIBK (0.7:1.3) mL]	100	65	65
5	2-propanol	38.5	11	29
6	H ₂ O:THF (1:4)	100	11	11
7	NMP	21	12	57
8	DMF	40	11.4	29
9	DMSO	96	72	75

Reaction conditions: 0.277 mmol (50 mg) fructose, 20 mg IBOMC, 160 °C, 1 h, in 3 mL various solvent systems. ^a HMF yield, and fructose conversion were calculated by HPLC using the calibration curve method.

Table S9: Catalyst optimization in fructose dehydration

Entry	IBOMC (mg)	Conversion (%) ^a	HMF yield (%) ^a	Selectivity (%)
1	10	81	59	72
2	20	96	72	75
3	30	97	67	70

Reaction conditions: 0.277 mmol (50 mg) fructose, 160 °C, 3 mL DMSO, 1 h, with different contents of IBOMC. ^a HMF yield and fructose conversion were calculated by HPLC using the calibration curve method.

Table S10: Solvent optimization for glucose dehydration

Entry	Solvent	Conversion (%) ^a	HMF yield (%) ^a	Selectivity (%)
1	Dumesic ^b	63	13	21
2 ^c	DMSO	36.5	11	30
3	H ₂ O:MIBK (1:2)	35.5	3.7	10
4	H ₂ O:ChCl:MIBK (1:1:2) ^d	- ^e	5	- ^e

Reaction conditions: 0.277 (50 mg) mmol glucose, 20 mg IBOMC, 160 °C, 3 h in 3 mL different solvent systems. ^a HMF yield, and glucose conversion were calculated by HPLC using the calibration curve method. ^b The Dumesic biphasic solvent: [H₂O: DMSO (0.3:0.7) mL / 2-Butanol: MIBK (0.7:1.3) mL]. ^c The reaction occurred in 6 h. ^d Weight ratio. ^e Not detected.

Table S11: Effect of H₂O and DMSO ratio in the queues phase of Dumesic solvent for glucose dehydration

Entry	DMSO : H ₂ O (mL)	Conversion (%) ^a	HMF yield (%) ^a	Selectivity (%)
1	0.3 : 0.7	70	6	8.5
2	0.5 : 0.5	74	14	19
3	0.7 : 0.3	95	45	47
4	0.8 : 0.2	100	12	12
5	1 : 0.0	36.5	11	30

Reaction conditions: 0.277 mmol (50 mg) glucose, 20 mg IBOMC, 160 °C, 6 h with various ratio of DMSO to H₂O of 3 mL Dumesic solvent system [DMSO/H₂O (volume ratio) + 2-butanol/MIBK (0.6 mL/ 1.4 mL)]. ^a HMF yield and glucose conversion were calculated by HPLC using the calibration curve method.

Table S12: Dehydration of sucrose and cellulose

Entry	Precursor (mg)	T (°C)	Conversion (%) ^a	HMF yield (%) ^a	Selectivity (%)
1	Sucrose (96)	160	100	40	40
2	Sucrose (96)	180	100	27	27
3	Cellulose (50)	160	70 ^b	<1	<1
4	Cellulose (50)	180	100 ^b	28	28

Reaction conditions: 0.277 mmol (0.96 mg) sucrose or 50 mg cellulose, 20 mg IBOMC as carbocatalyst in 3 mL Dumesic biphasic system and temperatures at 6 h; ^a Conversion and 5-HMF yield was determined by HPLC through the calibration curve method for sucrose. ^b Conversion was calculated with gravimetric method.

Table S13: Comparison between various catalysts in fructose dehydration

Entry	Catalyst	Solvent	Conversion (%) ^a	HMF yield (%) ^a	Selectivity (%)
1	IBOMC	Dumesic	100	65	65
2	NMCI	Dumesic	98	56	57
3	CMK-8	Dumesic	97	51	53
4	Carbon Active	Dumesic	89	43.5	49
5	IBOMC	DMSO	90	72	80
6	NMCI	DMSO	100	42	42
7	CMK-8	DMSO	52	30	57
8	Carbon Active	DMSO	80	17	21
9 ^b	IBOMC	DMSO	100	98	98
10 ^b	NMCI	DMSO	100	52	52
11 ^b	CMK-8	DMSO	93	40	43
12 ^b	Carbon Active	DMSO	100	37	37

Reaction conditions: 0.277 mmol (50 mg) fructose, 20 mg IBOMC, 3 mL solvent (DMSO or Dumesic solvent system [DMSO/H₂O (0.7 mL/0.3 mL) + 2-butanol/MIBK (0.6 mL/ 1.4 mL)]), 160 °C, 1 h. ^a HMF yield and fructose conversion were calculated by HPLC using the calibration curve method. ^b Reaction was occurred at 180 °C.

Table S14: Comparison between various carbocatalysts and IBOMC in dehydration of glucose at the same conditions

Entry	Catalyst	N%	Structure	Conversion (%) ^a	HMF yield (%) ^a	Selectivity (%)
1	IBOMC	11.2	3D-Cubic	95	45	47
2	CMK-8	0	3D-Cubic	66	7	11
3	Carbon Active	0	Disorder	80	4	1
4	NMCI	12.6	2D-Hexagonal	85	15	17

Reaction conditions: 0.277 mmol (50 mg) glucose, 20 mg catalyst, 3 mL Dumesic biphasic solvent system, 160 °C, 6 h; ^a HMF yield and glucose conversion were calculated by HPLC using the calibration curve method.

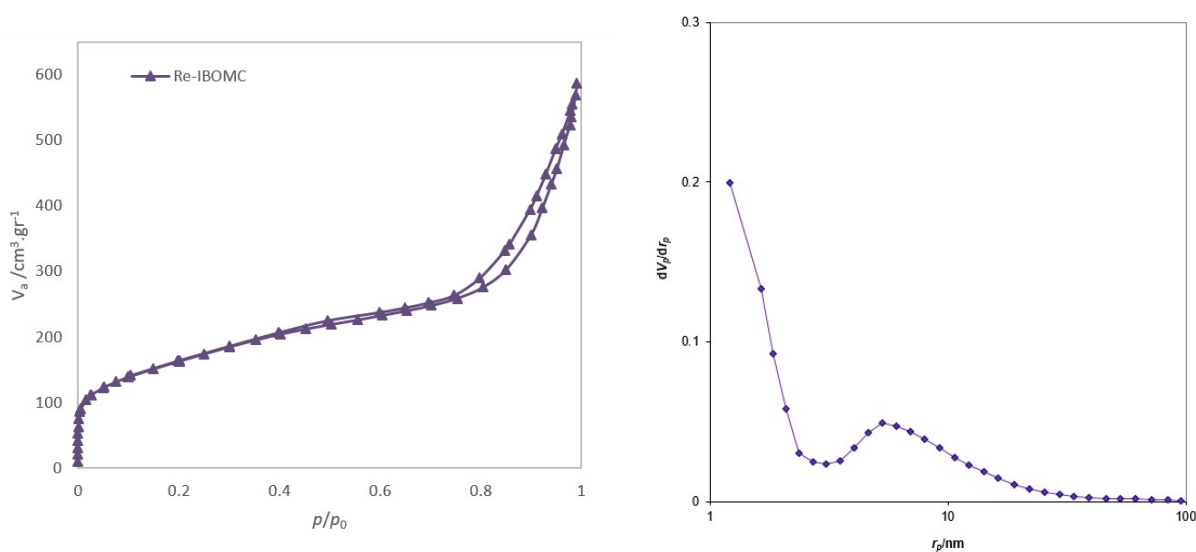


Figure S14: Porosimetry diagrams of recovered IBOMC

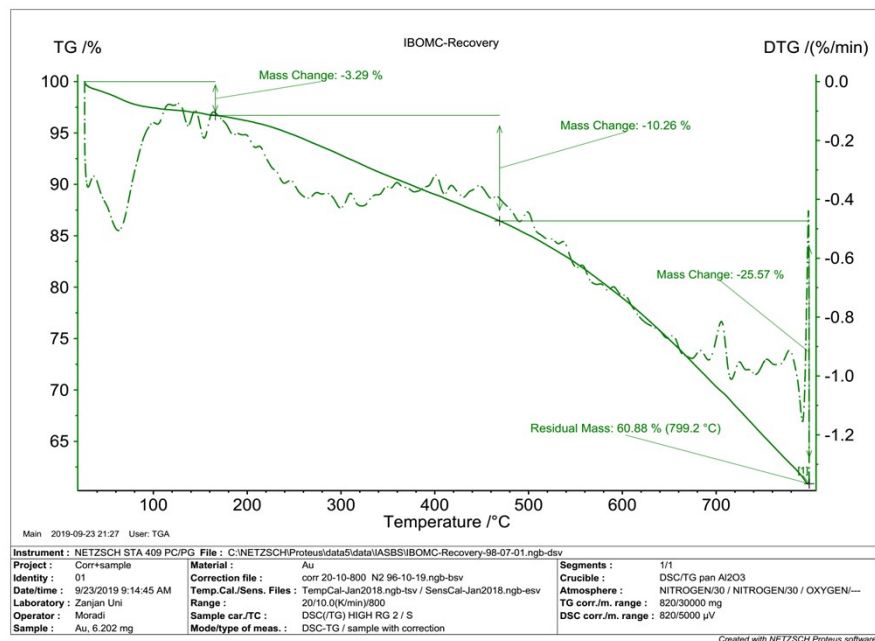


Figure S15: Thermal gravimetric analysis of recovered-IBOMC in dehydration of fructose into 5-HMF

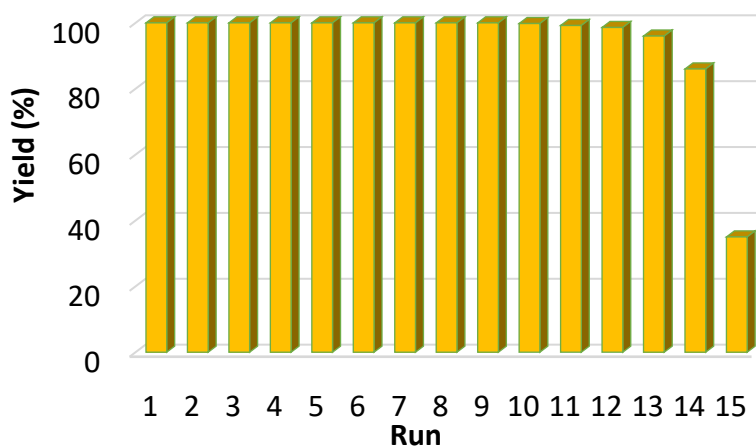


Figure S16: Reusability chart of IBOMC catalyst in the Knoevenagel condensation of benzaldehyde and malononitrile

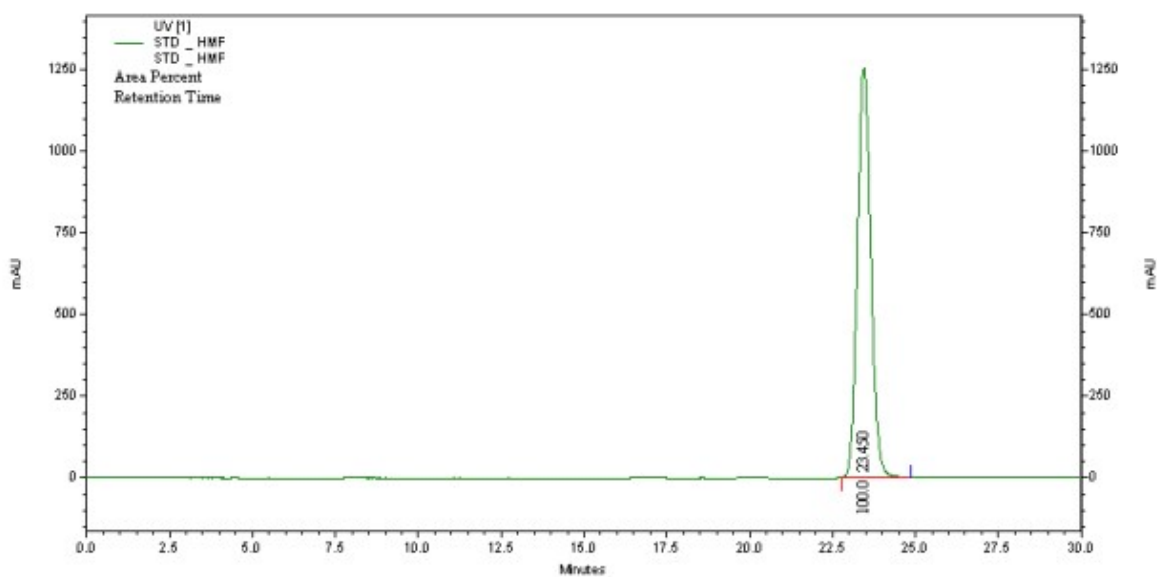
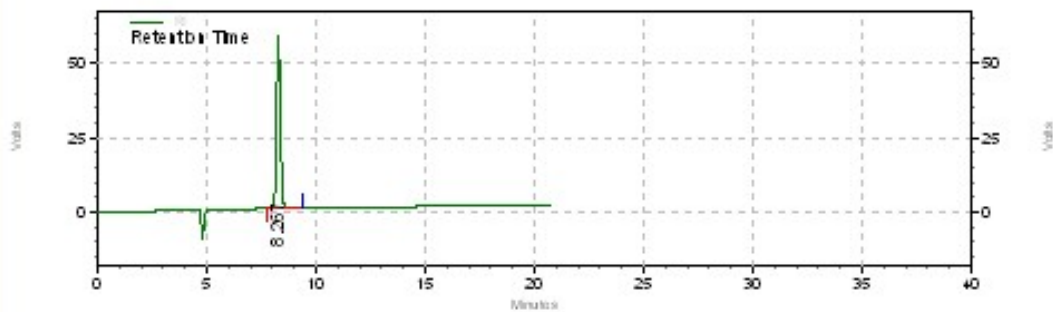


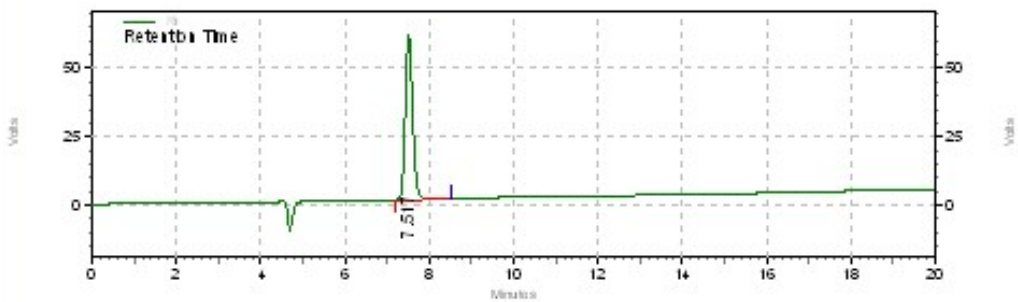
Figure S17: HPLC chromatogram of 5-HMF in Eurokat-H column



RI Results

Retention Time	Area	Area %	Height	Height %
8.267	702720	100.00	58008	100.00
Totals	702720	100.00	58008	100.00

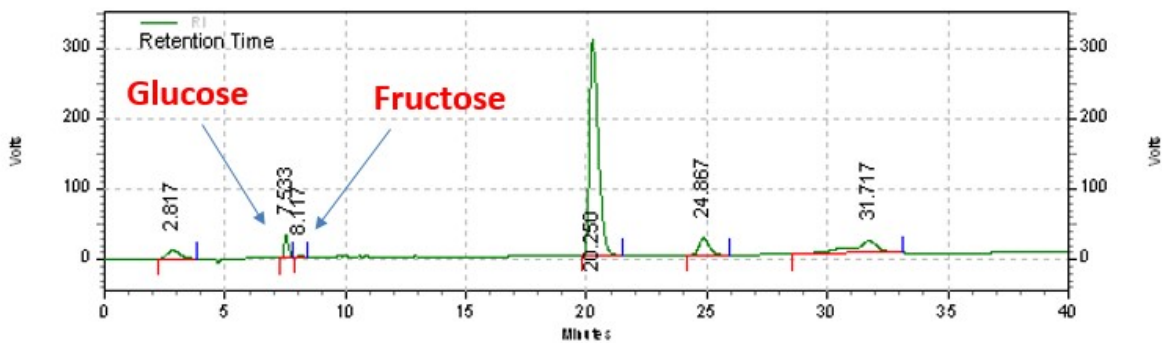
Figure S18: HPLC chromatogram of fructose in Eurokat-H column



RI Results

Retention Time	Area	Area %	Height	Height %
7.517	712221	100.00	59904	100.00
Totals	712221	100.00	59904	100.00

Figure S19: HPLC chromatogram of glucose in Eurokat-H column



RI Results

Retention Time	Area	Area %	Height	Height %
2.817	434299	4.03	11553	2.90
7.533	379682	3.52	31934	8.03
8.117	47801	0.44	3757	0.94
20.250	7741386	71.83	308670	77.58
24.867	699059	6.49	24231	6.09
31.717	1474674	13.68	17750	4.46

Totals	10776901	100.00	397895	100.00
--------	----------	--------	--------	--------

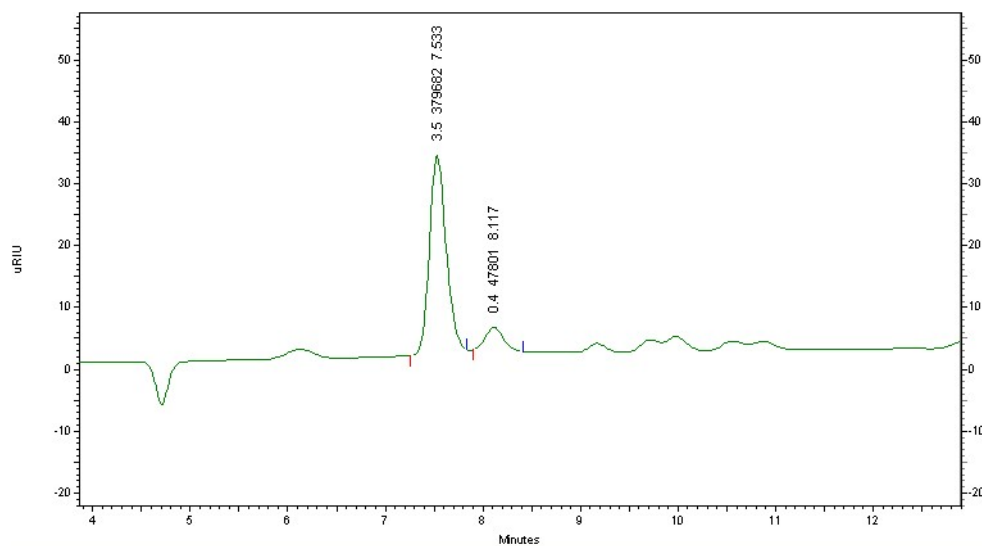
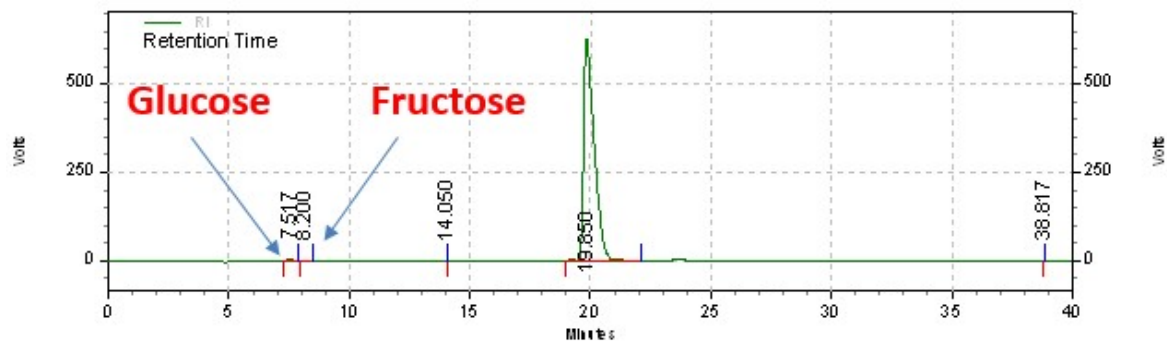


Figure S20: Detection of fructose through glucose dehydration with IBOMC as an acid-base bifunctional carbocatalyst



RI Results

Retention Time	Area	Area %	Height	Height %
7.517	52888	0.28	3771	0.60
8.200	11427	0.06	759	0.12
14.050	3	0.00	0	0.00
19.850	18976694	99.66	627207	99.28
38.817	1	0.00	0	0.00

Totals	19041013	100.00	631737	100.00
--------	----------	--------	--------	--------

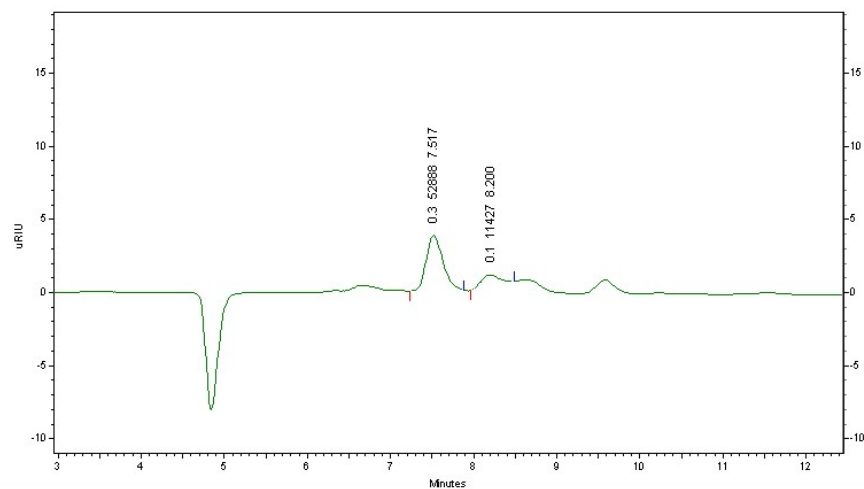


Figure S21: Detection of glucose through fructose dehydration with IBOMC as an acid-base bifunctional carbocatalyst

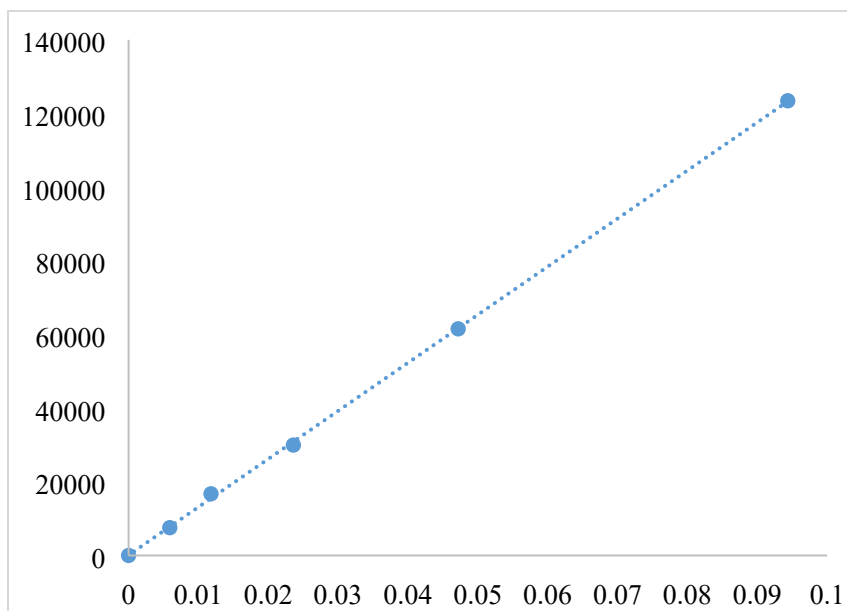


Figure S22: Fructose calibration curve. Stock solution included 0.051 g fructose in 3 mL H₂O, and every dilution was involved 50 µl of stock in 1 mL H₂O

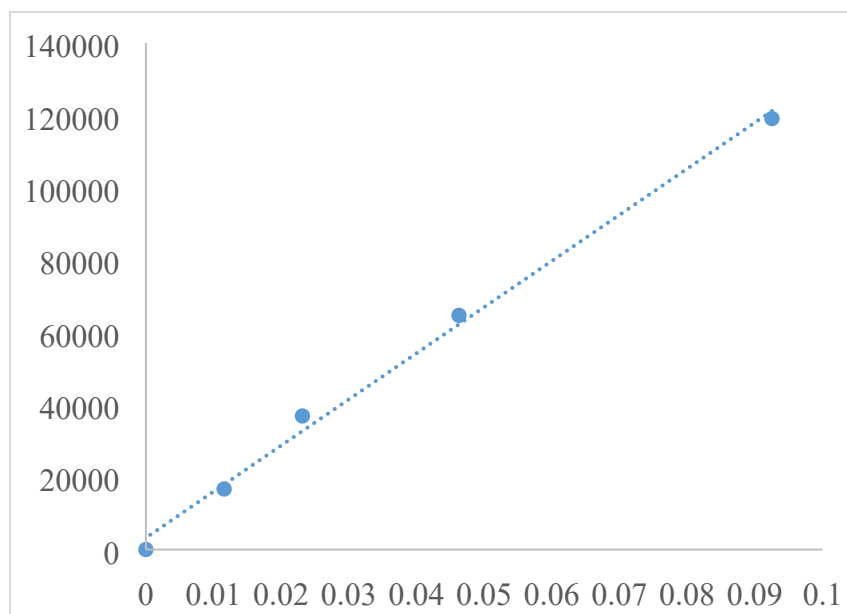


Figure S23: Glucose calibration curve. Stock solution: 0.05 g glucose in 3 mL H₂O, and every dilution was involved 50 µl of stock in 1 mL H₂O

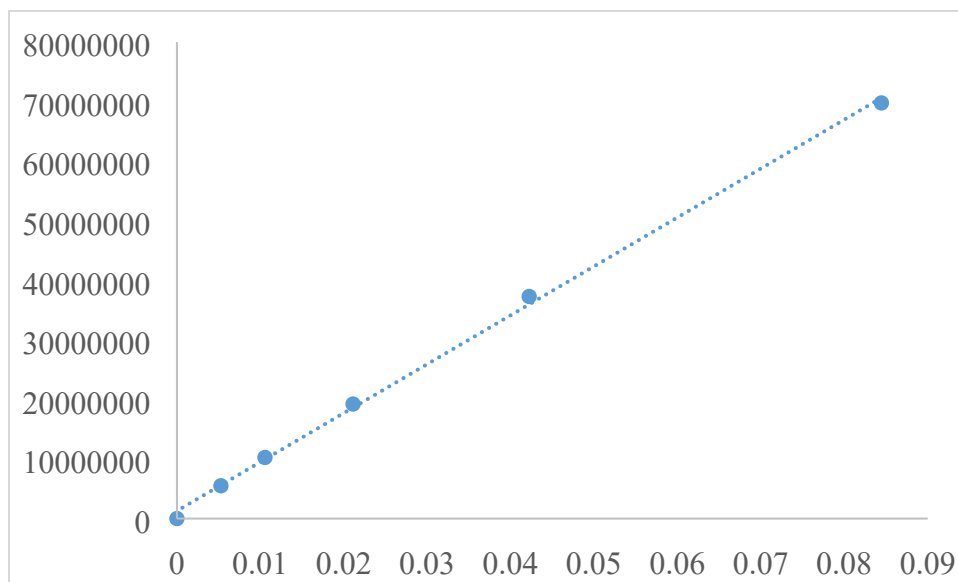


Figure S24: 5-HMF calibration curve-1. Stock solution included 0.036 g 5-HMF in 3.36 mL DMSO; every dilution was involved 50 μ l of solution in 1 mL H₂O

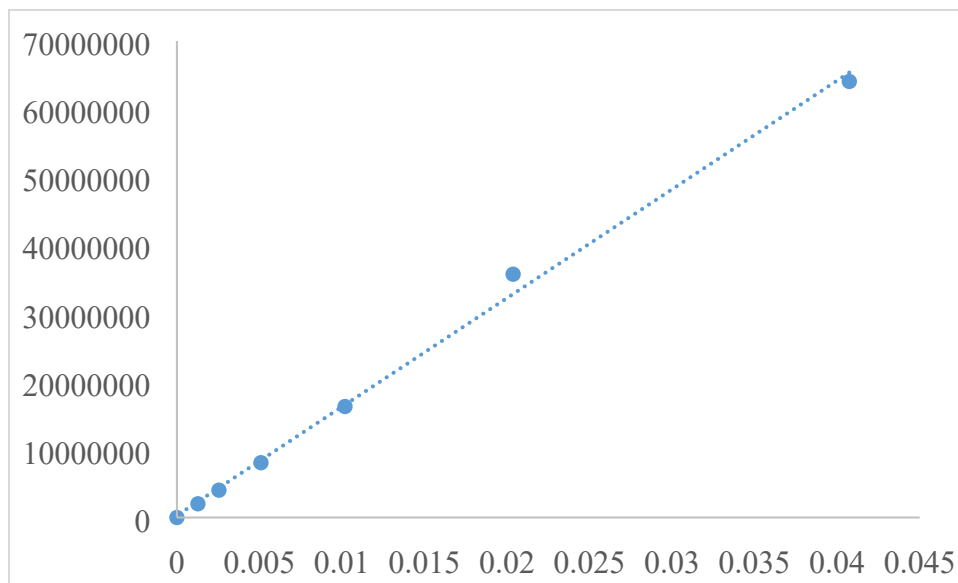
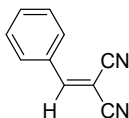


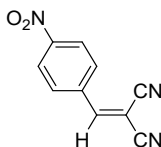
Figure S25: 5-HMF calibration curve-2. Stock solution included 0.0411 g 5-HMF in 1 mL H₂O; every dilution was involved 100 μ l of solution in 1 mL H₂O

2 Spectroscopic Data for Knoevenagel/deacetalization-Knoevenagel condensation Products

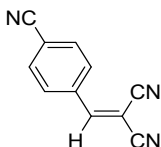
2-benzylidenemalononitrile: White solid; ^1H NMR (400 MHz, CDCl_3): $\delta_{\text{H}} = 7.95$ (2H, d, $J = 7.7$ Hz), 7.82 (1H, s), 7.66 (1H, m), 7.57 (2H, t, $J = 6$ Hz); ^{13}C NMR (100 MHz, CDCl_3): $\delta_{\text{C}} = 160.8$, 135.5, 131.7, 131.6, 130.5, 114.5, 113.4, 83.7.



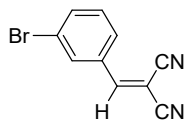
2-(4-nitrobenzylidene)malononitrile: Yellow solid; ^1H NMR (400 MHz, CDCl_3): $\delta_{\text{H}} = 8.45$ (2H, d, $J = 7.2$ Hz), 8.11 (2H, d, $J = 7.2$ Hz), 7.92 (1H, s); ^{13}C NMR (100 MHz, CDCl_3): $\delta_{\text{C}} = 157.7$, 151.2, 136.6, 132.1, 125.5, 113.4, 112, 4, 88.3.



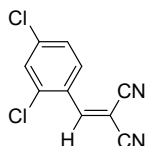
2-(4-cyanobenzylidene)malononitrile: Yellow solid; ^1H NMR (400 MHz, CDCl_3): $\delta_{\text{H}} = 8.03$ (2H, d, $J = 6.8$ Hz), 7.87 (1H, s), 7.85 (2H, d, $J = 6.8$ Hz); ^{13}C NMR (100 MHz, CDCl_3): $\delta_{\text{C}} = 158.1$, 135.0, 134.0, 131.5, 118.1, 117.1, 113.5, 112.5, 87.7.



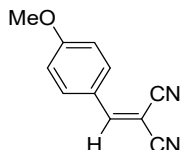
2-(3-bromobenzylidene)malononitrile: White solid; ^1H NMR (400 MHz, CDCl_3): $\delta_{\text{H}} = 8.02$ -7.99 (1H, m), 7.94-7.92 (1H, m), 7.80-7.77 (1H, m), 7.74 (1H, s), 7.46 (1H, t, $J = 8$ Hz); ^{13}C NMR (100 MHz, CDCl_3): $\delta_{\text{C}} = 158.9$, 138.1, 134.3, 133.4, 131.9, 129.4, 124.5, 114.0, 112.8, 85.5.



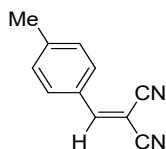
2-(2,4-dichlorobenzylidene)malononitrile: White solid; ^1H NMR (400 MHz, CDCl_3): $\delta_{\text{H}} = 8.22$ (1H, s), 8.18 (1H, d, $J = 8.4$ Hz), 7.60 (1H, d, $J = 2.4$ Hz), 7.46 (1H, dd, $J_1 = 8.4$, $J_2 = 2.4$ Hz); ^{13}C NMR (100 MHz, CDCl_3): $\delta_{\text{C}} = 155.4$, 141.9, 138.0, 131.6, 130.9, 129.2, 128.3, 113.8, 112.6, 86.8.



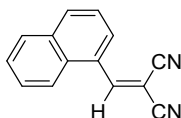
2-(4-methoxybenzylidene)malononitrile: White solid; $^1\text{H NMR}$ (400 MHz, CDCl_3): $\delta_{\text{H}} = 7.95$ (2H, d, $J = 9.2$ Hz), 7.70 (1H, s), 7.05 (2H, d, $J = 9.2$ Hz), 4(3H, s); $^{13}\text{C NMR}$ (100 MHz, CDCl_3): $\delta_{\text{C}} = 165.6, 159.7, 134.3, 124.8, 116.0, 115.3, 114.2, 79.4, 56.6$.



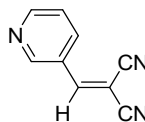
2-(4-Methylbenzylidene)malononitrile: White solid; $^1\text{H NMR}$ (400 MHz, CDCl_3): $\delta_{\text{H}} = 7.85$ (2H, d, $J = 8$ Hz), 7.75 (1H, s), 7.37 (2H, d, $J = 8$ Hz), 2.49 (3H, s); $^{13}\text{C NMR}$ (100 MHz, CDCl_3): $\delta_{\text{H}} = 160.6, 147.2, 131.7, 131.2, 129.3, 114.8, 113.7, 82.0, 22.9$.



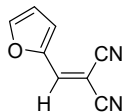
2-(naphthalen-1-ylmethylene)malononitrile: White solid; $^1\text{H NMR}$ (400 MHz, CDCl_3): $\delta_{\text{H}} = 8.70$ (1H, s), 8.35 (1H, d, $J = 7.6$ Hz), 8.15 (1H, d, $J = 8$ Hz), 8.00 (2H, d, $J = 8$ Hz), 7.75-7.63 (3H, m); $^{13}\text{C NMR}$ (100 MHz, CDCl_3): $\delta_{\text{C}} = 157.7, 134.9, 133.5, 131.1, 129.4, 128.6, 128.5, 127.5, 127.3, 125.4, 122.3, 113.7, 112.5, 85.2$.



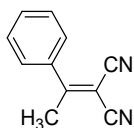
2-(3-pyridylmethylene)malononitrile: Yellow solid; $^1\text{H NMR}$ (400 MHz, CDCl_3): $\delta_{\text{H}} = 8.93$ (1H, s), 8.87-8.85 (1H, m), 8.53-8.51 (1H, m), 7.86 (1H, s), 7.58-7.55 (1H, m); $^{13}\text{C NMR}$ (100 MHz, CDCl_3): $\delta_{\text{C}} = 156.4, 154.6, 152.4, 135.6, 124.3, 112.9, 111.9, 85.7, 77.3$.



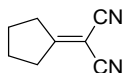
2-(furan-2-ylmethylene)malononitrile: Red solid; $^1\text{H NMR}$ (400 MHz, CDCl_3): $\delta_{\text{H}} = 7.85$ (1H, d, $J = 1.6$ Hz), 7.55 (1H, s), 7.40 (1H, d, $J = 3.6$ Hz), 6.75-6.73 (1H, m); $^{13}\text{C NMR}$ (100 MHz, CDCl_3): $\delta_{\text{C}} = 150.4, 148.9, 143.9, 124.4, 115.3, 114.7, 113.4, 78.3$.



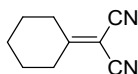
2-(1-phenylethylidene)malononitrile: White solid; ^1H NMR (400 MHz, CDCl_3): $\delta_{\text{H}} = 7.59\text{--}7.54$ (5H, m), 2.7 (3H, s); ^{13}C NMR (100 MHz, CDCl_3): $\delta_{\text{C}} = 175.5, 135.9, 132.3, 129.1, 127.3, 112.8, 112.7, 84.7, 24.3$.



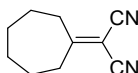
2-Cyclopentylidenemalononitrile: Colorless liquid; ^1H NMR (400 MHz, CDCl_3): $\delta_{\text{H}} = 2.86\text{--}2.82$ (4H, m), 2.00-1.94 (4H, m); ^{13}C NMR (100 MHz, CDCl_3): $\delta_{\text{C}} = 192.3, 111.7, 81.4, 36.2, 26.0$.



2-Cyclohexylidenemalononitrile: Colorless liquid; ^1H NMR (400 MHz, CDCl_3): $\delta_{\text{H}} = 2.7$ (4H, m), 1.84-1.79 (4H, m), 1.69-1.66 (2H, m); ^{13}C NMR (100 MHz, CDCl_3): $\delta_{\text{C}} = 185.2, 111.7, 82.4, 34.7, 27.9, 25.0$.



2-Cycloheptylidenemalononitrile: Colorless liquid; ^1H NMR (400 MHz, CDCl_3): $\delta_{\text{H}} = 2.86\text{--}2.83$ (4H, m), 1.84-1.79 (4H, m), 1.66-1.61 (4H, m); ^{13}C NMR (100 MHz, CDCl_3): $\delta_{\text{C}} = 188.5, 111.9, 85.0, 36.3, 29.0, 26.2$.



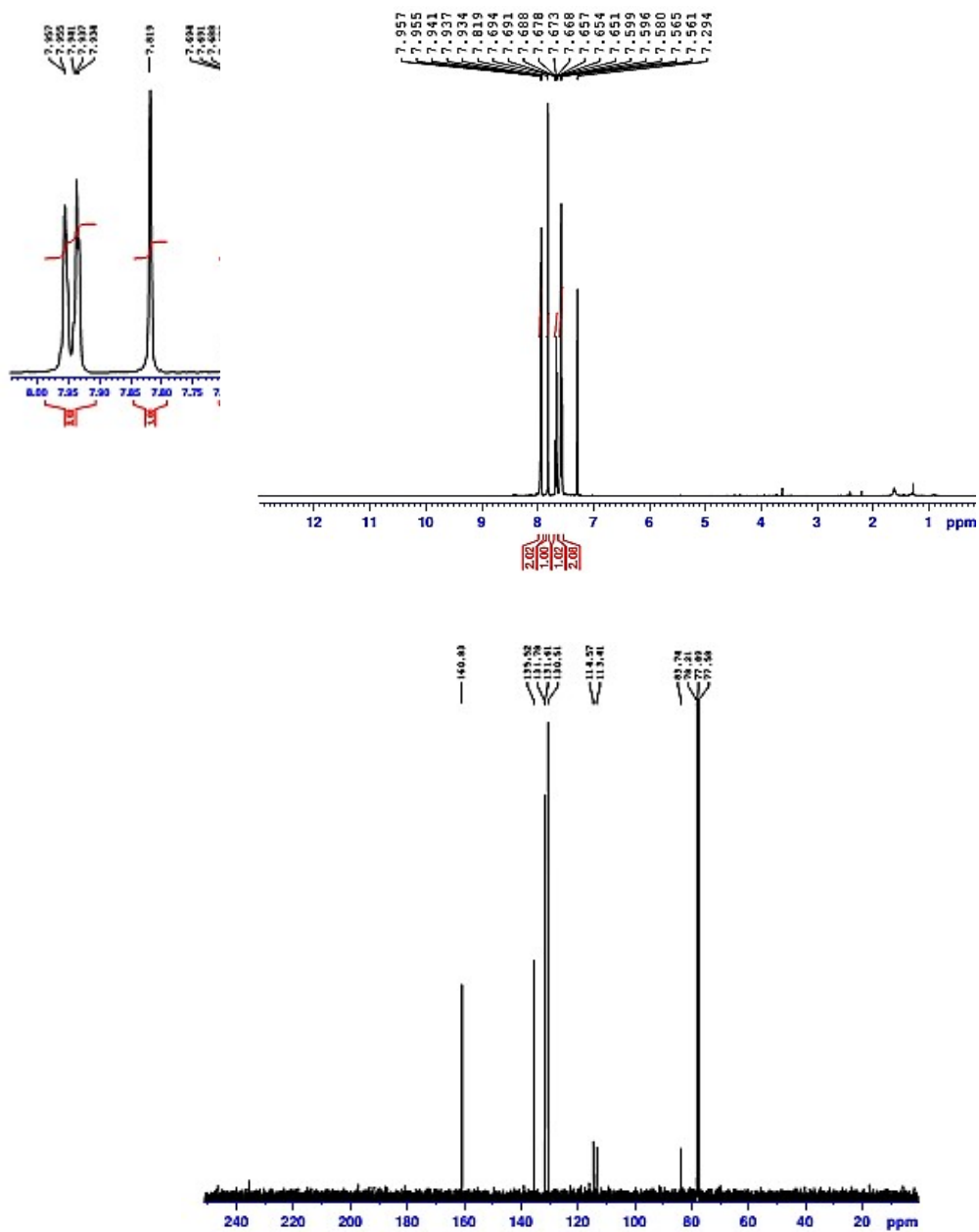
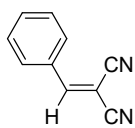


Figure S26: $^1\text{H-NMR}$ and $^{13}\text{C-NMR}$ spectra of the 2-benzylidenemalononitrile product in CDCl_3

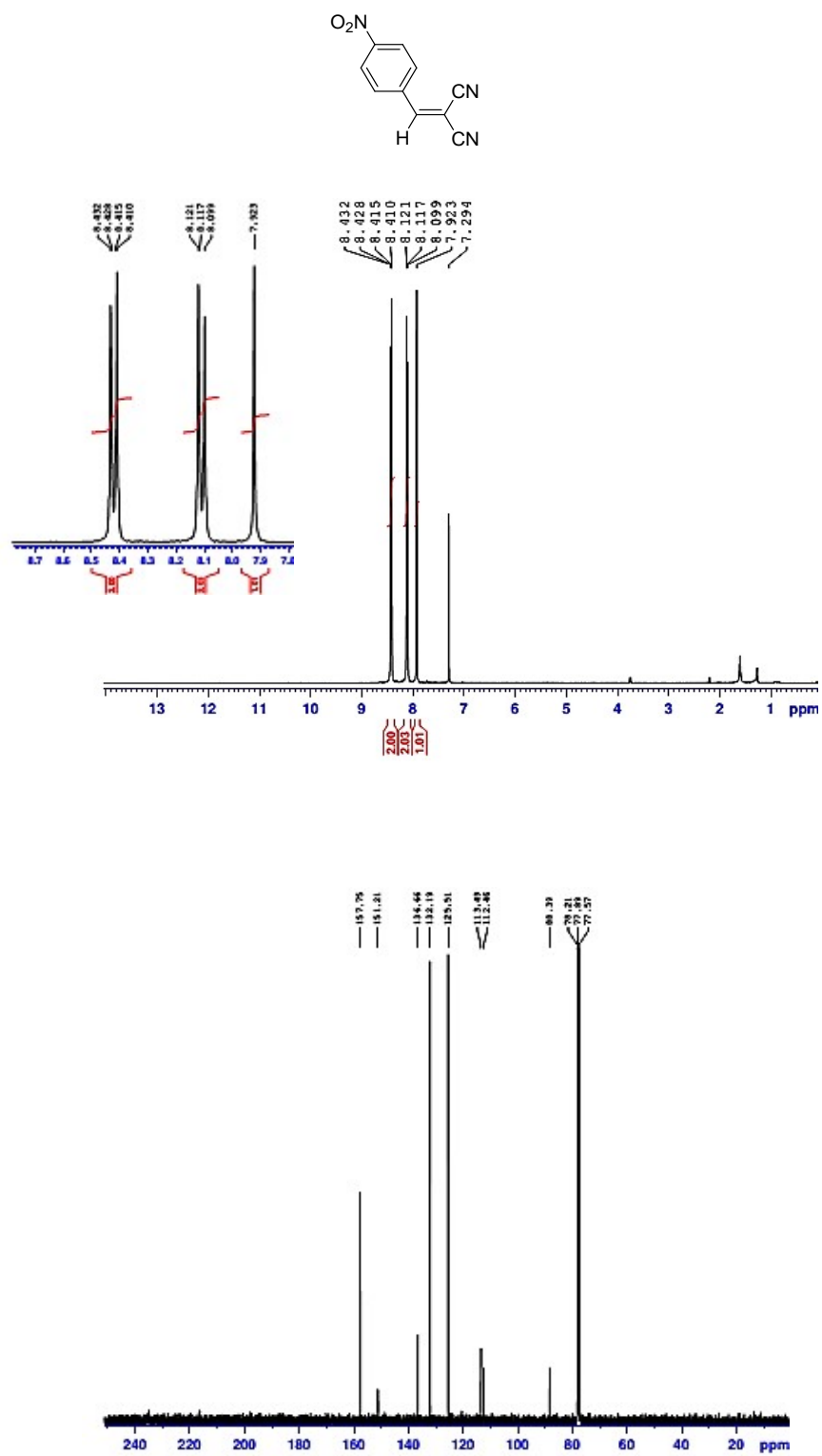


Figure S27: ¹H-NMR and ¹³C-NMR spectra of the 2-(4-nitrobenzylidene)malononitrile product in CDCl₃

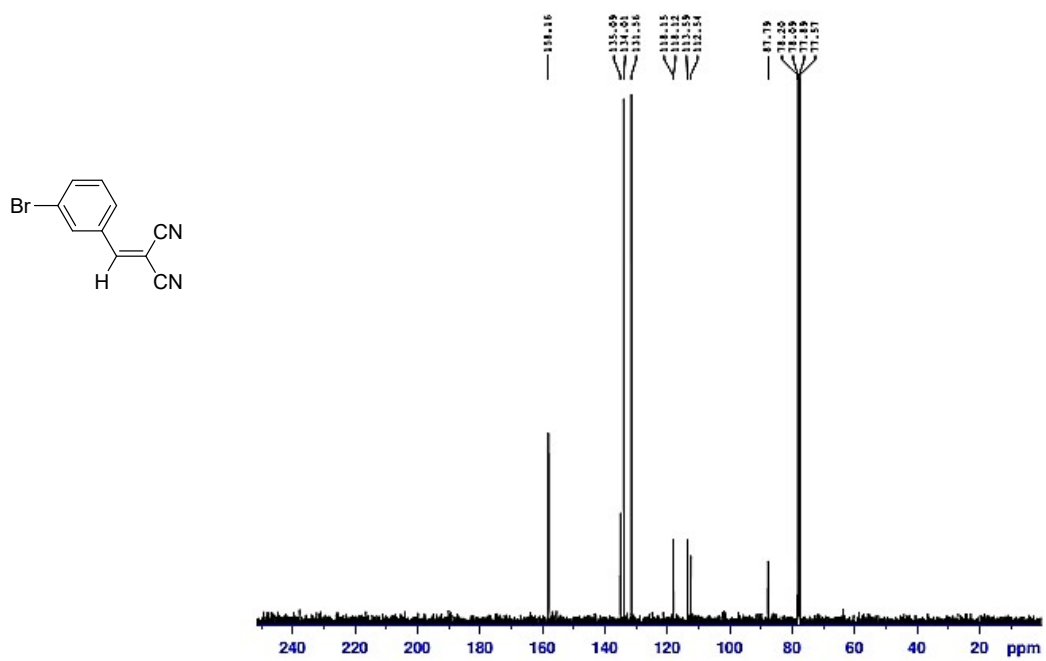
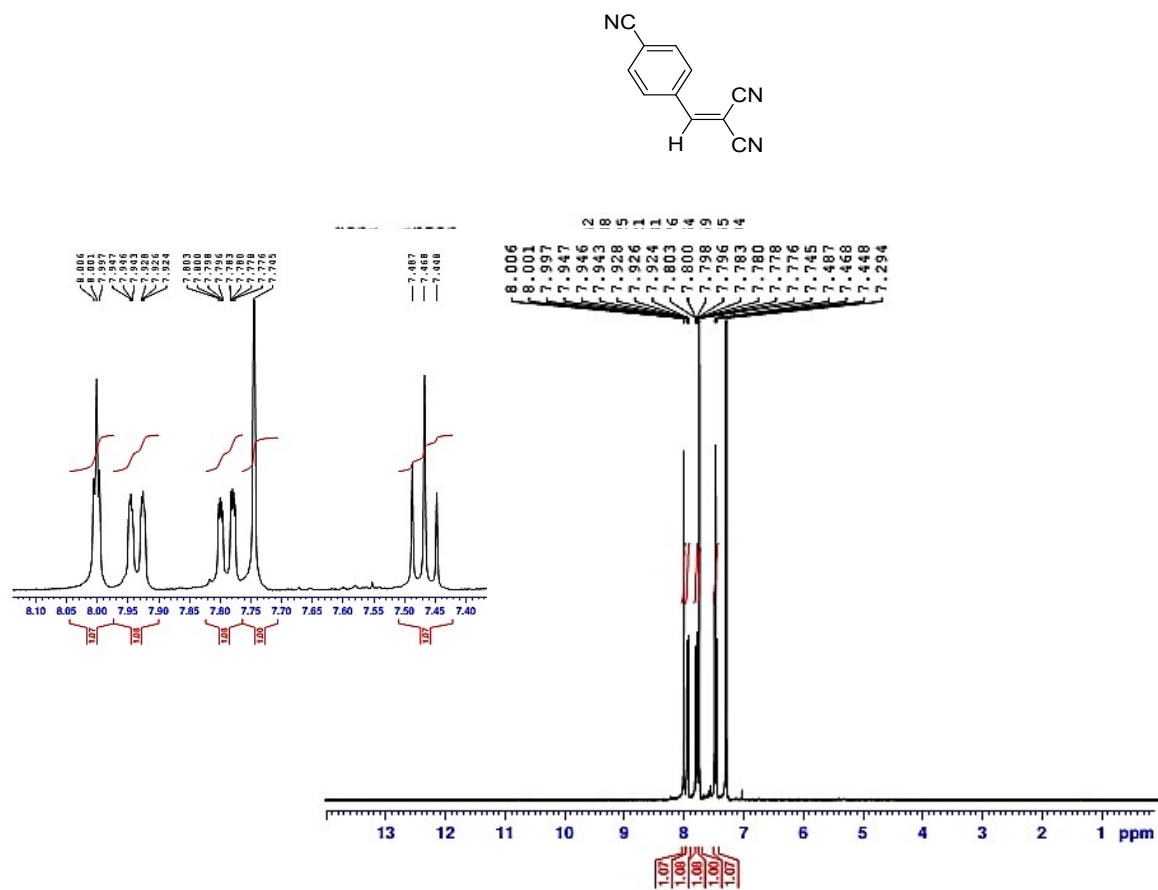


Figure S28: ¹H-NMR and ¹³C-NMR spectra of the 2-(4-cyanobenzylidene)malononitrile product in CDCl₃

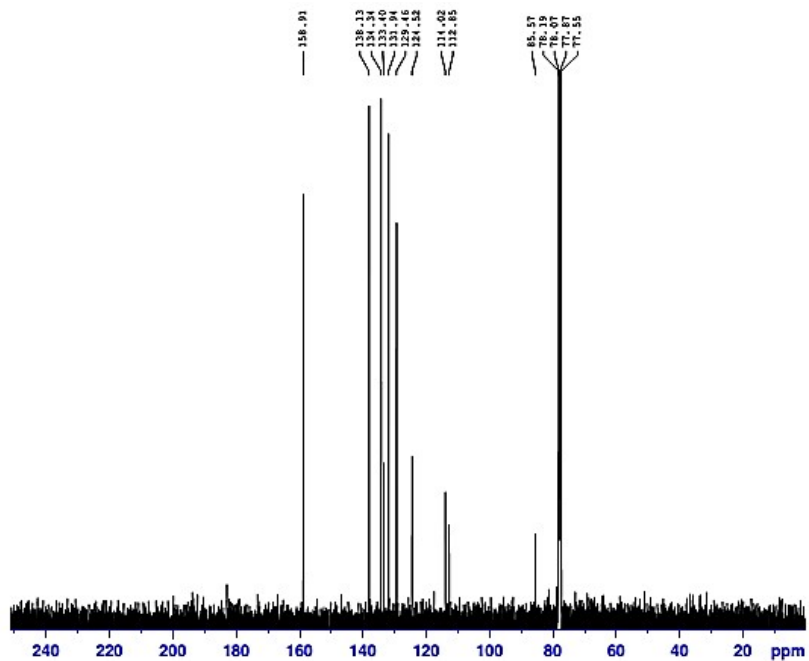
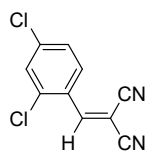


Figure S29: ^1H -NMR and ^{13}C -NMR spectra of the 2-(3-bromobenzylidene)malononitrile product in CDCl_3



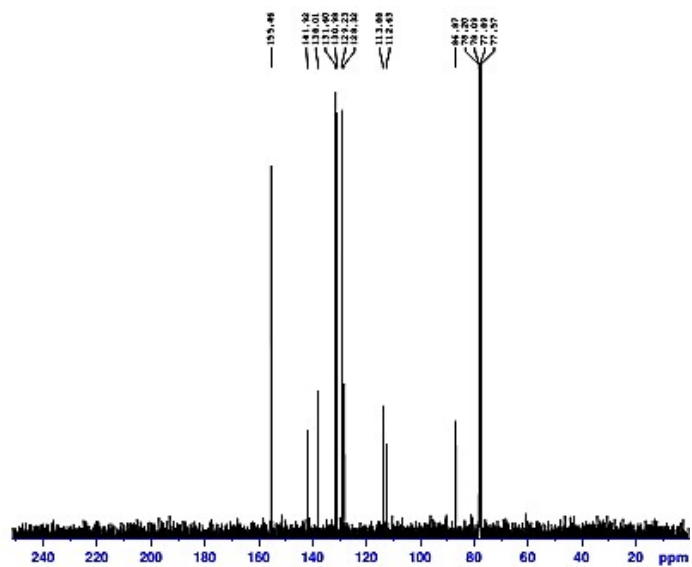
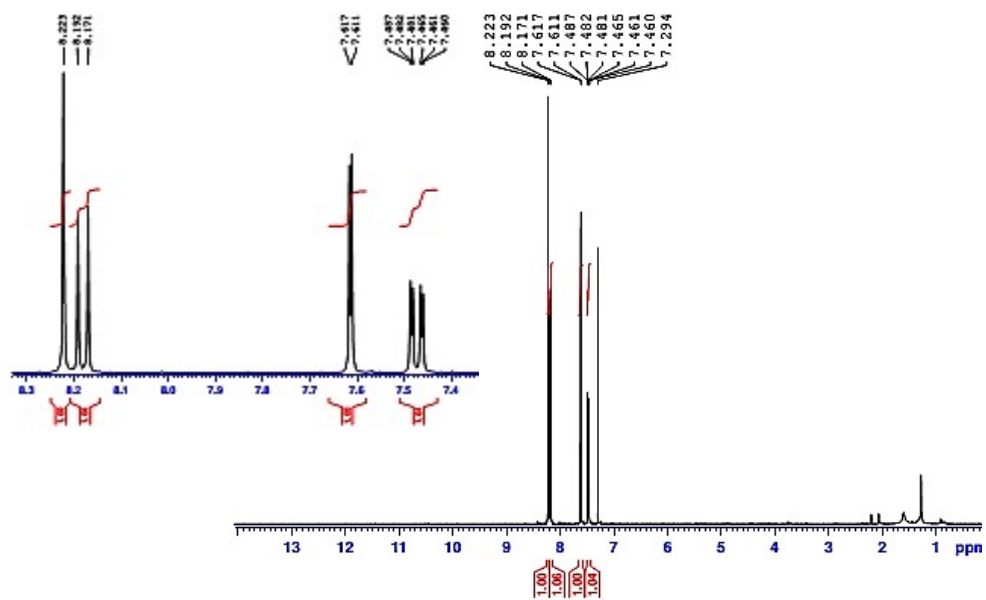


Figure S30: ^1H -NMR and ^{13}C -NMR spectra of the 2-(2,4-dichlorobenzylidene)malononitrile product in CDCl_3

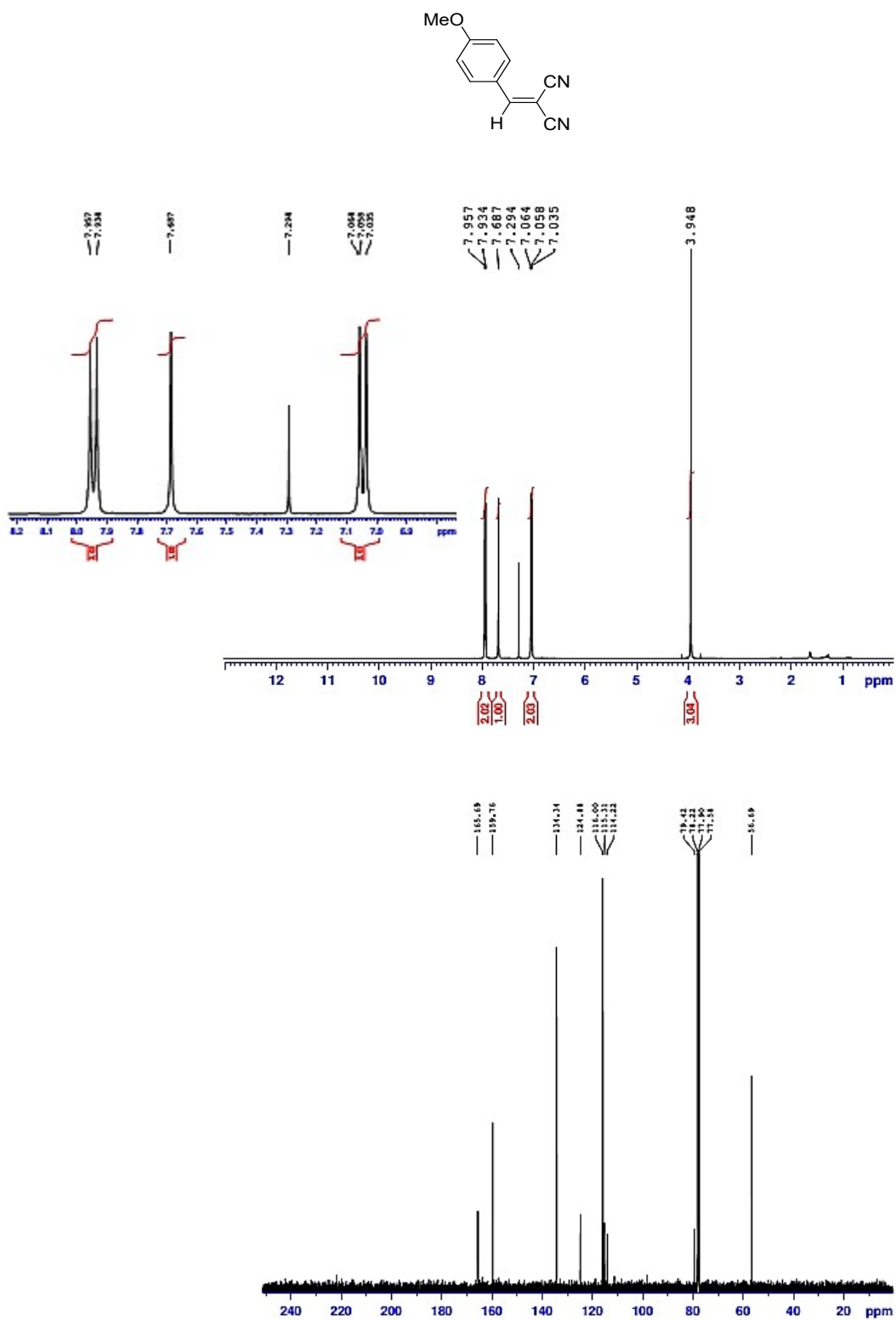


Figure S31: ¹H-NMR and ¹³C-NMR spectra of the 2-(4-methoxybenzylidene)malononitrile product in CDCl₃

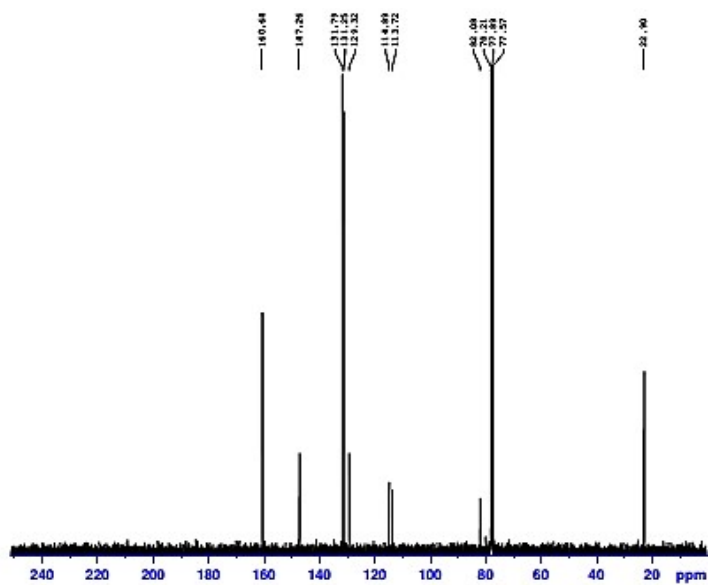
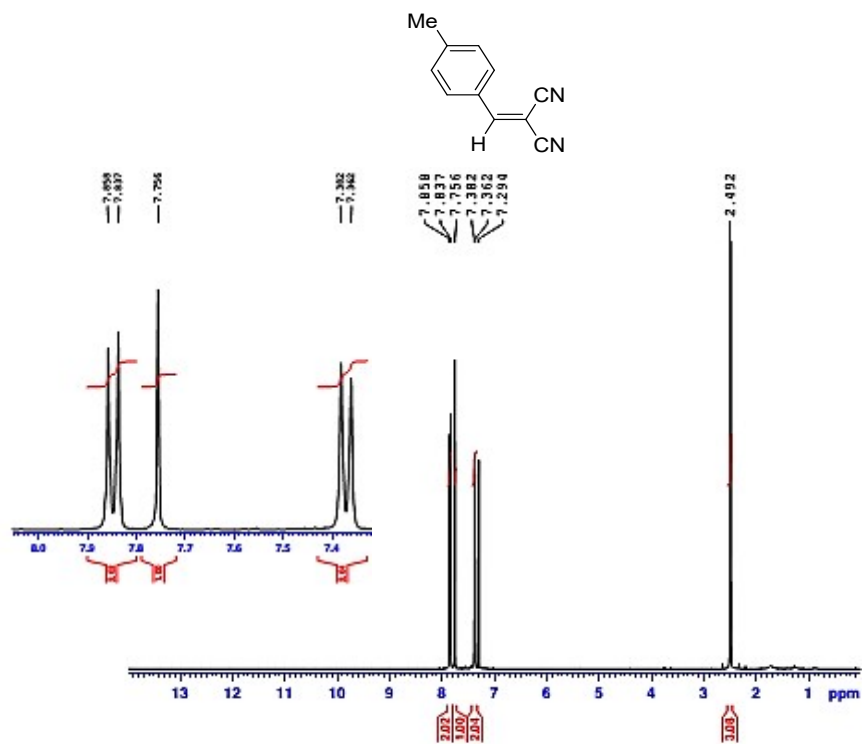


Figure S32 : ¹H-NMR and ¹³C-NMR spectra of the 2-(4-methylbenzylidene)malononitrile product in CDCl₃

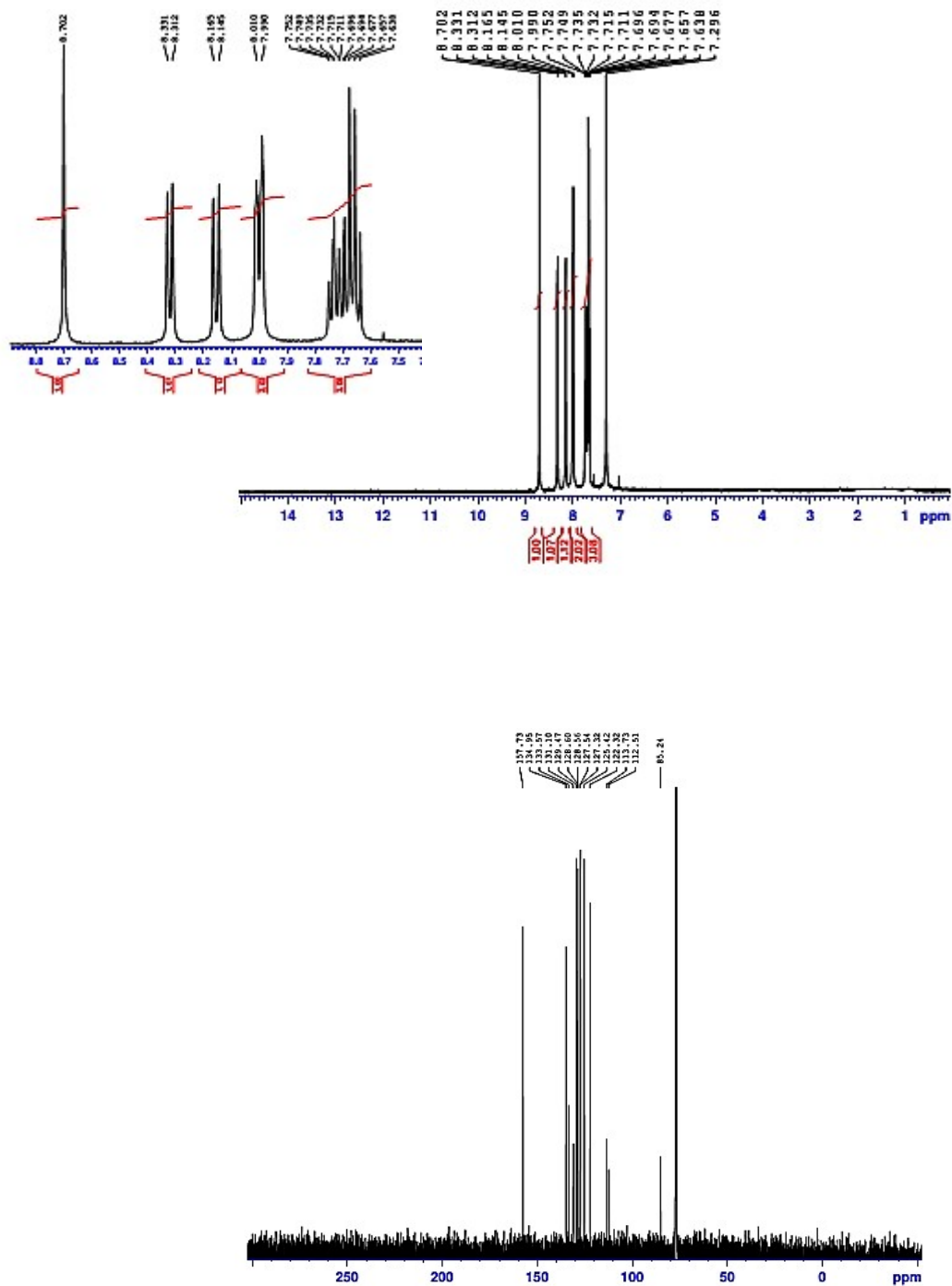
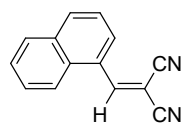


Figure S33: ¹H-NMR and ¹³C-NMR spectra of the 2-(naphthalen-1-ylmethylene)malononitrile product in CDCl₃

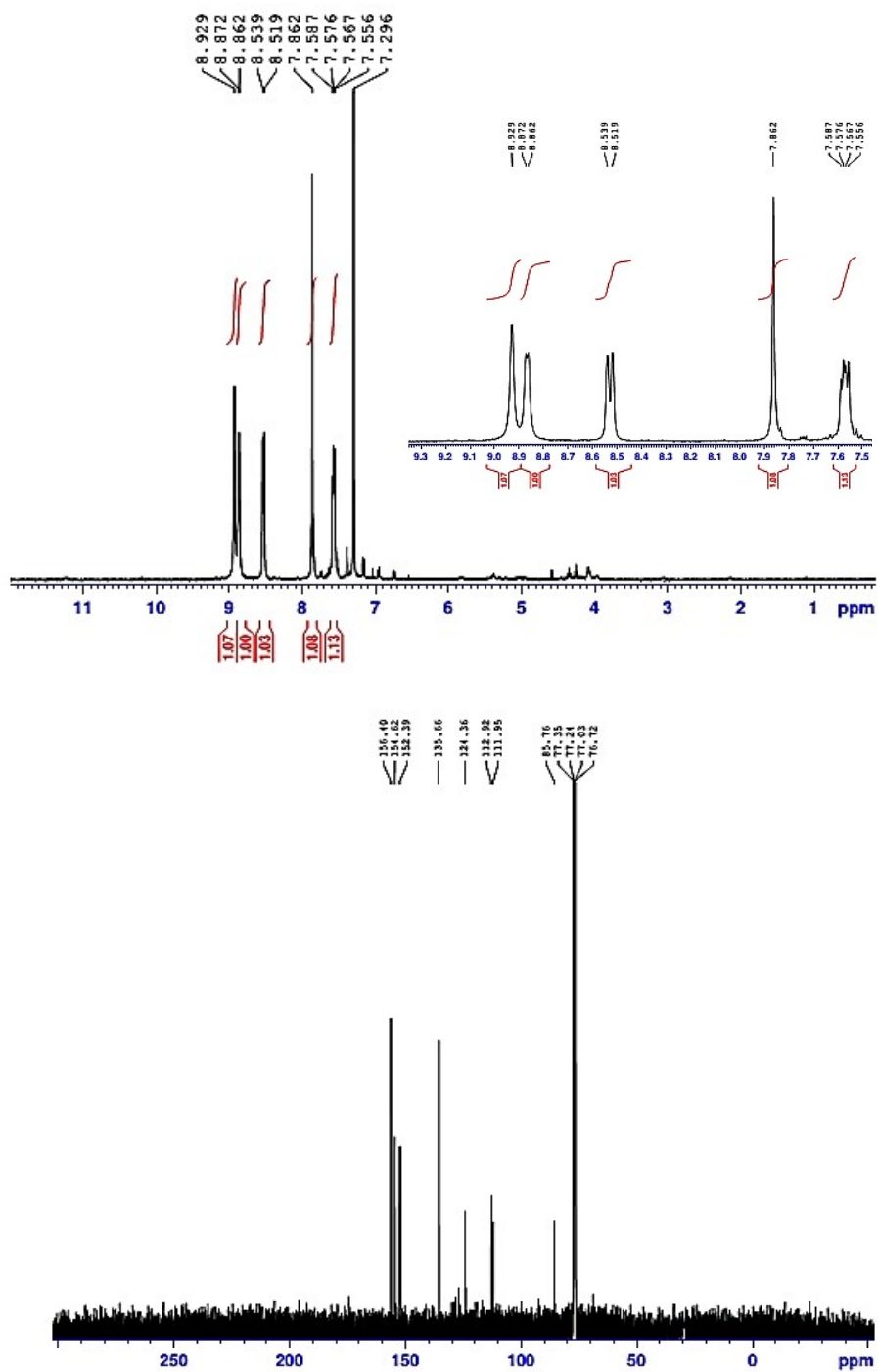
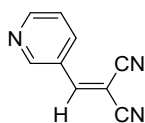


Figure S34: $^1\text{H-NMR}$ and $^{13}\text{C-NMR}$ spectra of the 2-(3-pyridylmethylene)malononitrile product in CDCl_3

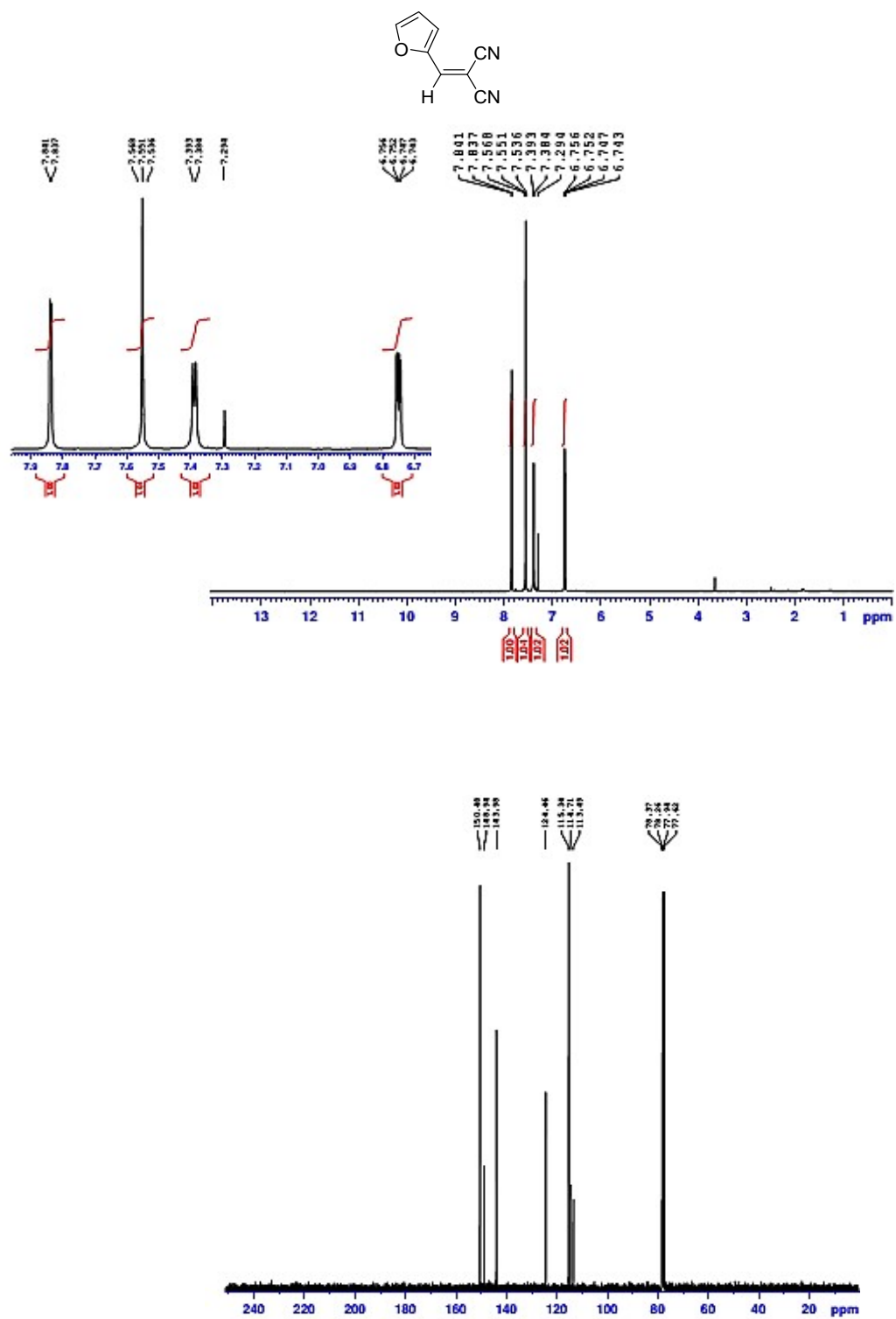


Figure S35: ¹H-NMR and ¹³C-NMR spectra of the 2-(furan-2-ylmethylene)malononitrile product in CDCl₃

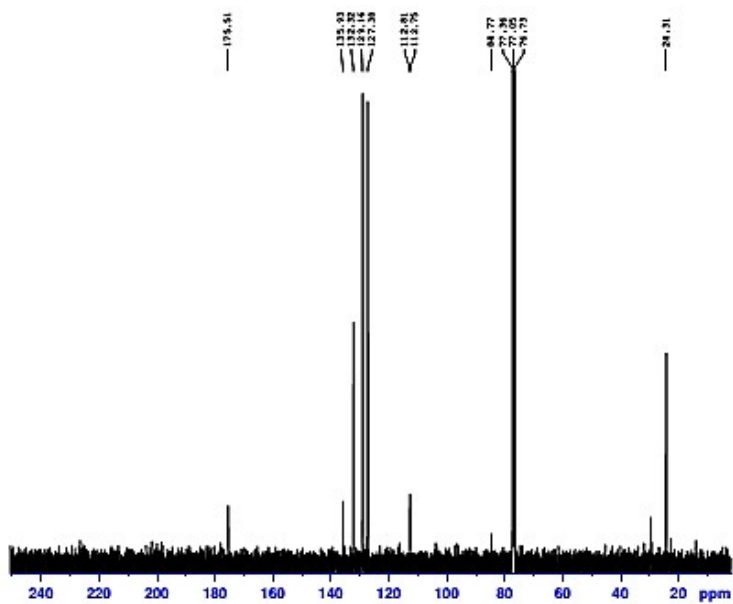
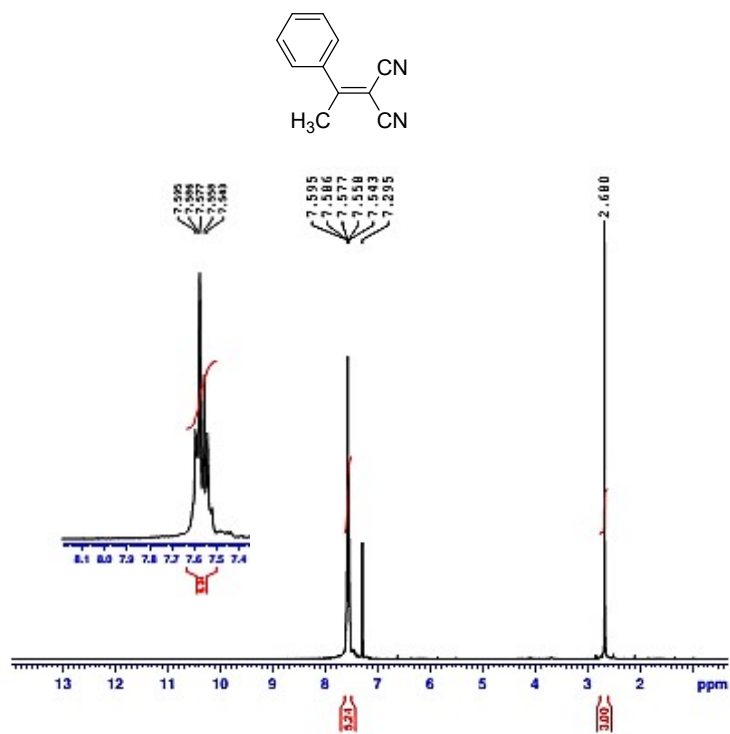


Figure S36: ¹H-NMR and ¹³C-NMR spectra of the 2-(1-phenylethylidene)malonitrile product in CDCl₃

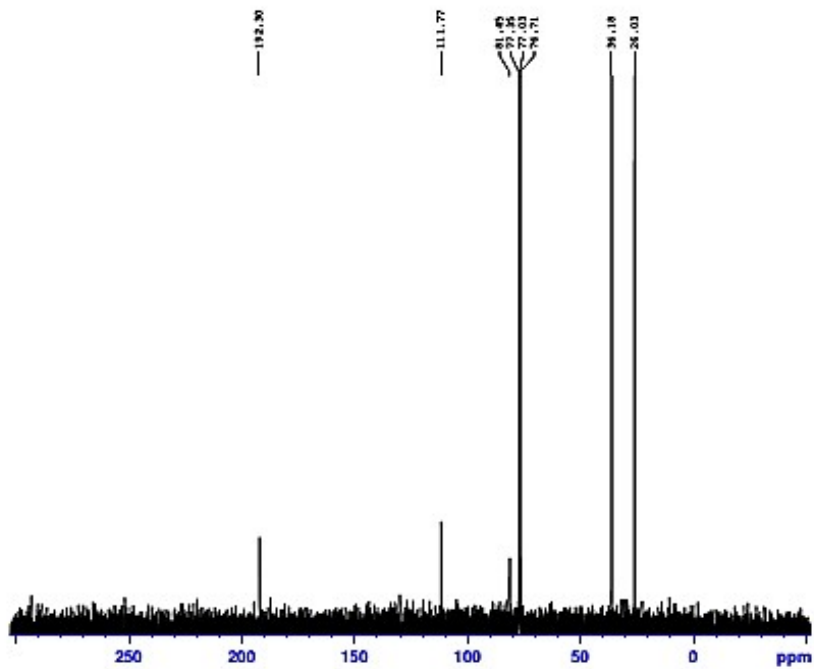
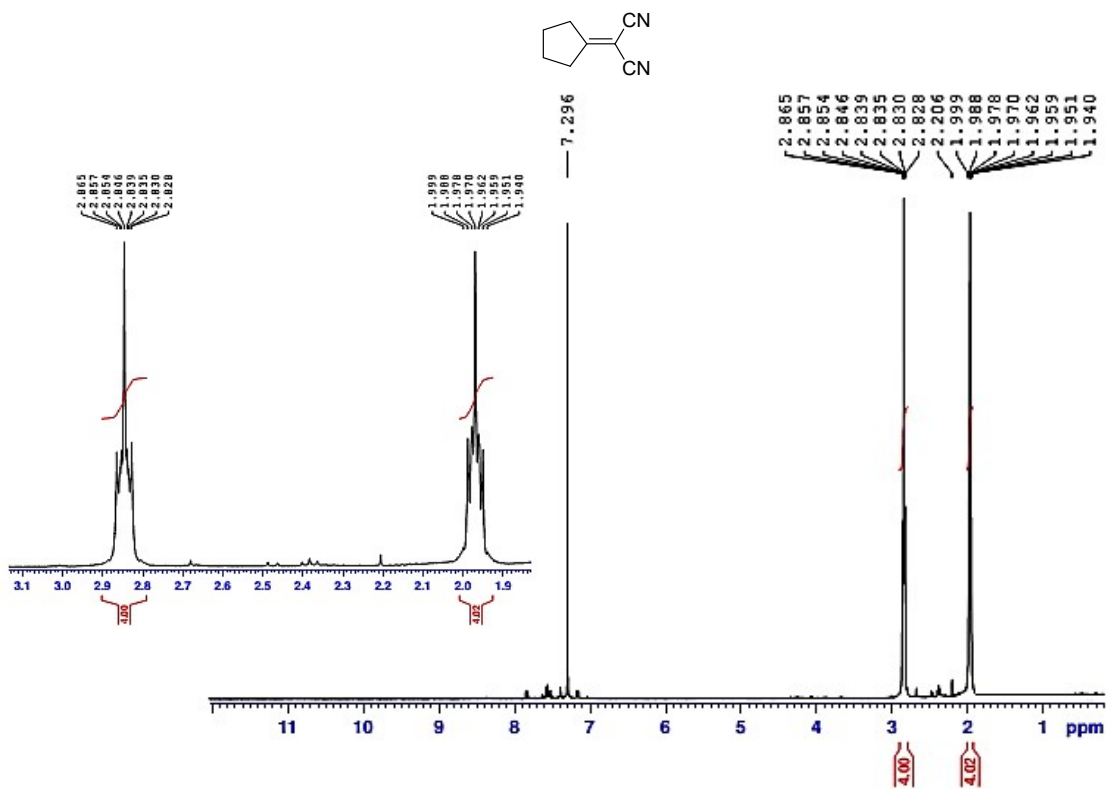


Figure S37: ¹H-NMR and ¹³C-NMR spectra of the 2-cyclopentylidene-1,1-dicyanoethane product in CDCl₃

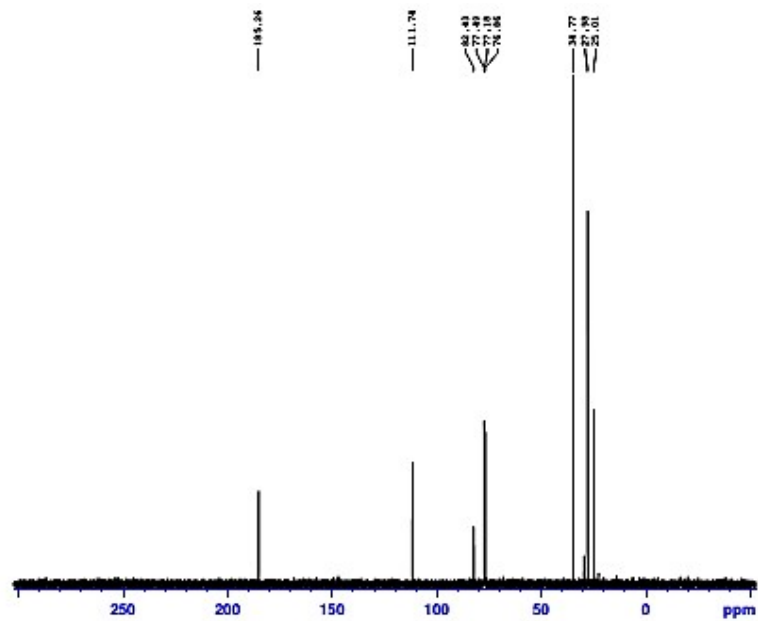
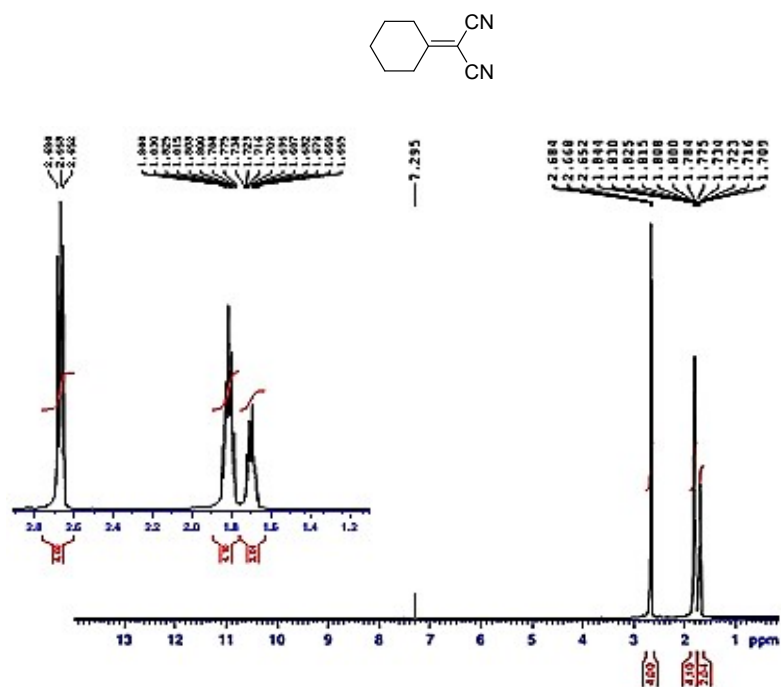


Figure S38: ¹H-NMR and ¹³C-NMR spectra of the 2-cyclohexylidene malononitrile product in CDCl₃

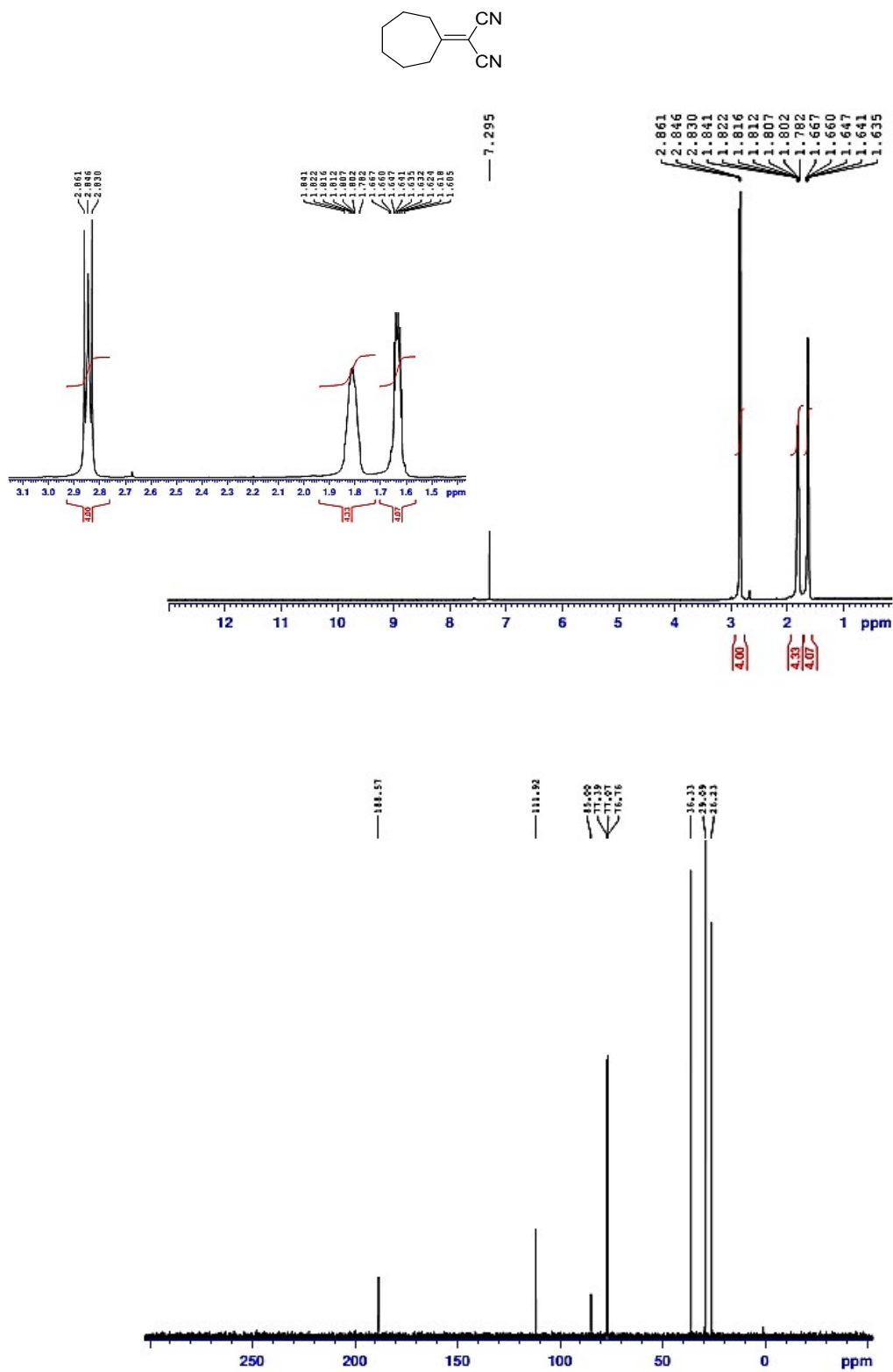


Figure S39: ¹H-NMR and ¹³C-NMR spectra of the 2-cycloheptylidene malononitrile product in CDCl₃

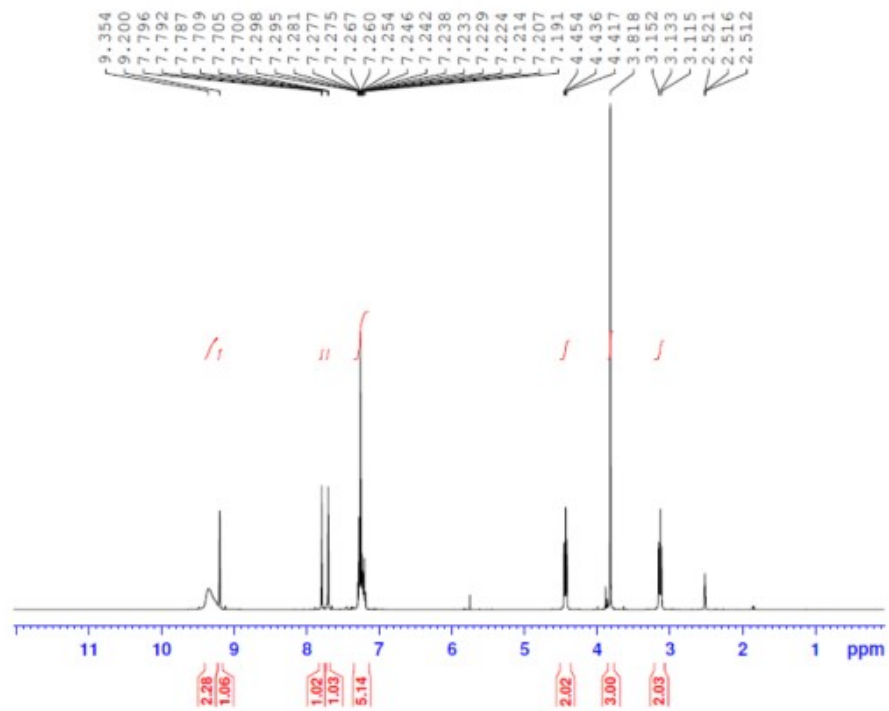


Figure S40: ^1H -NMR spectrum (400 MHz, CDCl_3) of 1-methyl-3-phenethyl-*1H*-imidazolium hydrogen sulfate (MPIHS)

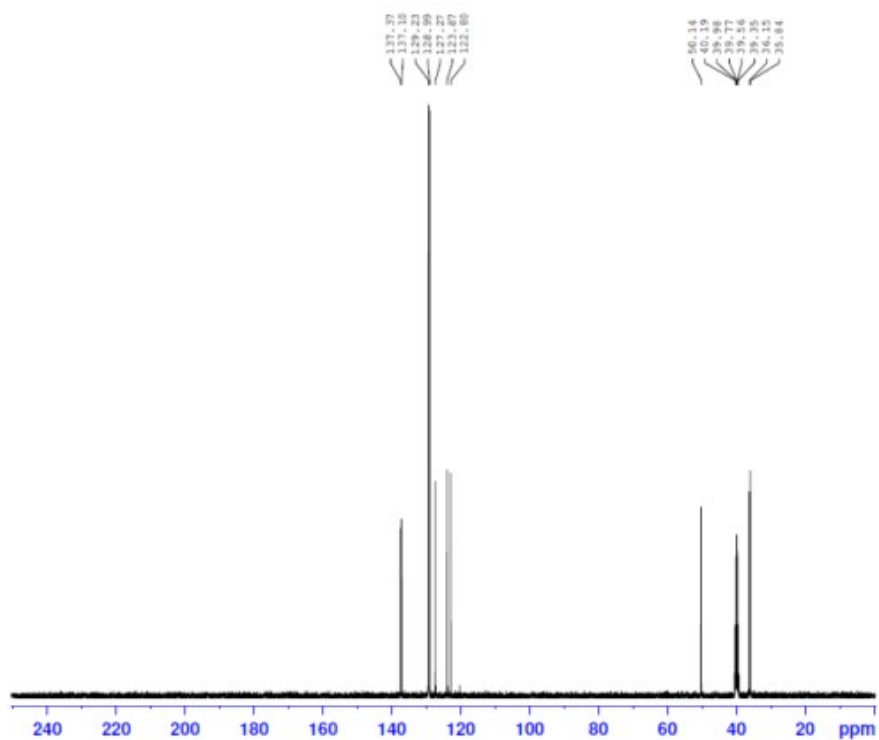


Figure S41: ^{13}C -NMR spectrum (100 MHz, DSMO-d_6) of 1-methyl-3-phenethyl-*1H*-imidazolium hydrogen sulfate (MPIHS)

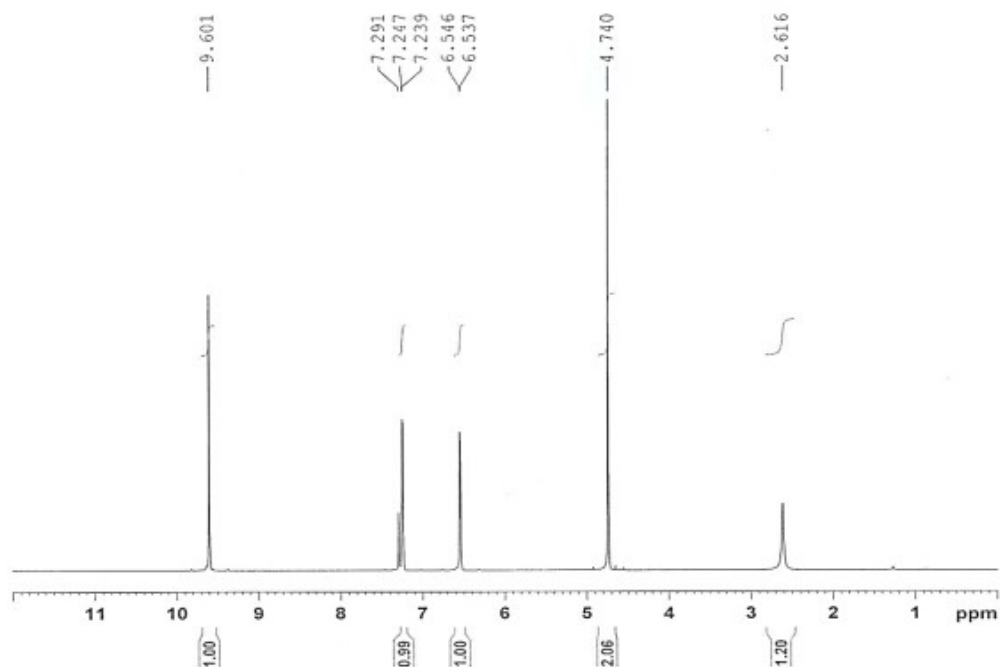


Figure S42: ^1H -NMR spectrum (400 MHz, CDCl_3) of 5-HMF

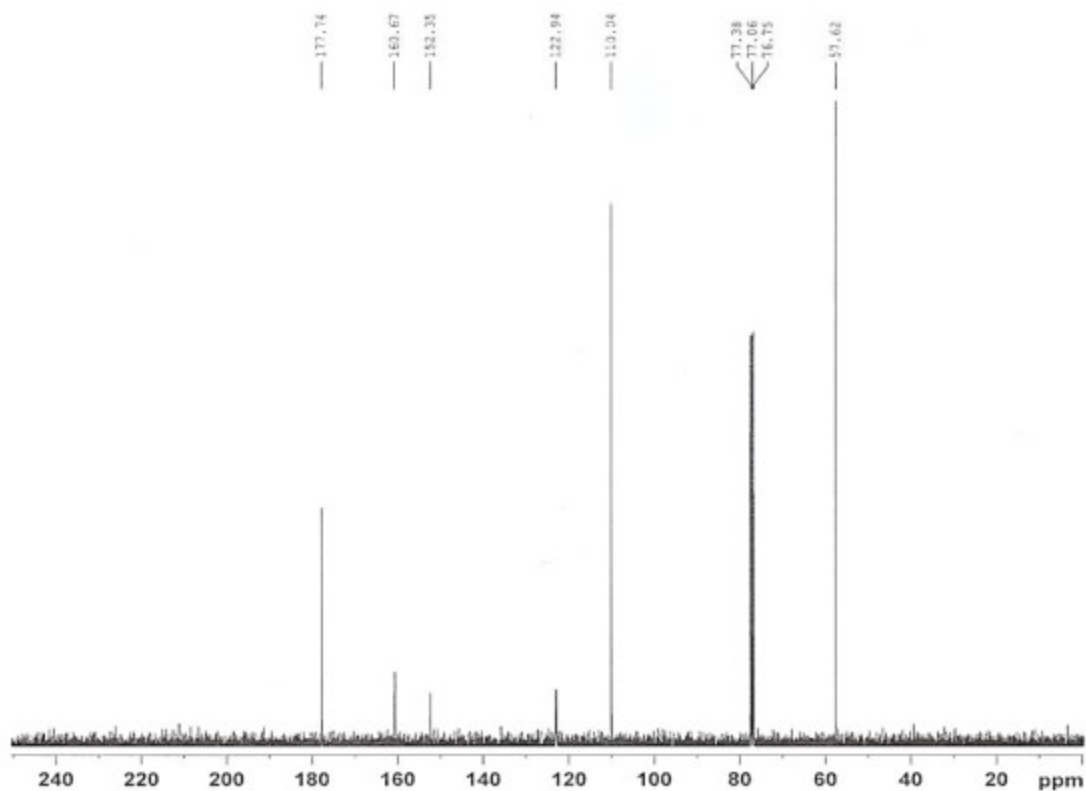


Figure S43: ^{13}C -NMR spectrum (100 MHz, CDCl_3) of 5-HMF

3 References

1. F. Kleitz, S. H. Choi and R. Ryoo, *Chemical Communications*, 2003, 2136-2137.
2. D. Zhao, J. Feng, Q. Huo, N. Melosh, G. H. Fredrickson, B. F. Chmelka and G. D. Stucky, *science*, 1998, **279**, 548-552.
3. B. Karimi, H. Barzegar and H. Vali, *Chemical Communications*, 2018, **54**, 7155-7158.
4. S. Jun, S. H. Joo, R. Ryoo, M. Kruk, M. Jaroniec, Z. Liu, T. Ohsuna and O. Terasaki, *Journal of the American chemical society*, 2000, **122**, 10712-10713.